

Model selection-based estimation for generalized additive models using mixtures of g-priors: Towards systematization

Gyeonghun Kang¹ and Seonghyun Jeong^{*1,2}

¹Department of Statistics and Data Science, Yonsei University, Seoul, Korea

²Department of Applied Statistics, Yonsei University, Seoul, Korea

January 26, 2023

Abstract

We consider estimation of generalized additive models using basis expansions with Bayesian model selection. Although Bayesian model selection is an intuitively appealing tool for regression splines caused by the flexible knot placement and model-averaged function estimates, its use has traditionally been limited to Gaussian additive regression, as posterior search of the model space requires a tractable form of the marginal model likelihood. We introduce an extension of the method to distributions belonging to the exponential family using the Laplace approximation to the likelihood. Although the Laplace approximation is successful with all Gaussian-type prior distributions in providing a closed-form expression of the marginal likelihood, there is no broad consensus on the best prior distribution to be used for nonparametric regression via model selection. We observe that the classical unit information prior distribution for variable selection may not be suitable for nonparametric regression using basis expansions. Instead, our study reveals that mixtures of g-priors are more suitable. A large family of mixtures of g-priors is considered for a detailed examination of how various mixture priors perform in estimating generalized additive models. Furthermore, we compare several priors of knots for model selection-based spline approaches to determine the most practically effective scheme. The model selection-based estimation methods are also compared with other Bayesian approaches to function estimation. Extensive simulation studies demonstrate the validity of the model selection-based approaches. We provide an R package for the proposed method.

Keywords: Bayesian nonparametrics; exponential family models; mixtures of g-priors; nonparametric regression; regression splines.

1 Introduction

Since its inception, the generalized additive model (GAM) has played a significant role in statistics and machine learning, and has received a great deal of attention from many theorists and practitioners (e.g., [Yee and Mitchell, 1991](#); [Yee and Wild, 1996](#); [Guisan et al., 2002](#); [McLean et al., 2014](#); [Wood et al., 2015](#)). The GAM is seen as an interpretable semiparametric compromise between

*Corresponding author: sjeong@yonsei.ac.kr

the parametric generalized linear model (GLM) and fully nonparametric regression with multidimensional smoothing. More specifically, the GAM explains the relationship between multiple predictor variables and a (possibly non-Gaussian) response variable by employing an additive structure of univariate functions (Hastie and Tibshirani, 1986). Therefore, at the expense of the flexibility of multidimensional smoothing, the GAM provides a straightforward interpretation of the amount each predictor variable contributes to the mean response as a univariate function.

A variety of estimation procedures have been proposed for nonparametric regression and additive models from frequentist and Bayesian perspectives. Focusing on the Bayesian philosophy, typical techniques for univariate smooth function estimation include Gaussian process priors (Williams and Rasmussen, 1995), Bayesian P-splines (Lang and Brezger, 2004), and basis expansion methods with model selection (Smith and Kohn, 1996; Denison et al., 1998a; DiMatteo et al., 2001). As a branch of Bayesian estimation methods, basis expansion with Bayesian model selection (BMS), which we call the BMS-based approach to nonparametric regression, enjoys appealing theoretical properties and successful empirical performances (Smith and Kohn, 1996; Denison et al., 1998a; DiMatteo et al., 2001; Rivoirard and Rousseau, 2012; De Jonge and Van Zanten, 2012; Shen and Ghosal, 2015). Specifically, BMS-based approaches determine intrinsic basis terms by comparing Bayes factors based on BMS, which translates to choosing more plausible basis terms among a possible set of candidates in a data-driven manner. Apart from univariate function estimation, BMS-based approaches are often useful for multidimensional smoothing problems such as Bayesian multivariate adaptive regression splines (MARS) (Denison et al., 1998b) and Bayesian additive regression trees (BART) (Chipman et al., 2010).

Although BMS-based methods are conceptually simple, they can be computationally successful only when the calculation of the marginal likelihood, obtained by marginalizing the regression coefficients out, is readily accessible. This has typically restricted the use of BMS for nonparametric regression to Gaussian nonparametric regression only. For GLMs and GAMs, marginalization is often unachievable unless a conjugate prior is used for the coefficients; however, such a conjugate prior does not provide a convenient form of the marginal likelihood (Chen and Ibrahim, 2003). The sole accessible application may be nonparametric probit regression (e.g., Jeong et al., 2017; Sohn et al., 2022), which has a convenient expression with latent variables (Albert and Chib, 1993). If marginalization is not analytically tractable, BMS-based methods require numerical marginalization of the coefficients through Markov chain Monte Carlo (MCMC) algorithms, such as the reversible jump MCMC (Green, 1995). These are often far more inefficient than using Bayes factors, unless a sound proposal distribution is available (Al-Awadhi et al., 2004). This difficulty partially leads to the prevalence of the P-spline-based Bayesian methods for estimation in GAMs during the early stages of their development (e.g., Fahrmeir and Lang, 2001; Brezger and Lang, 2006).

One natural solution to this issue is considering an approximation to the likelihood, such as the Laplace approximation, so that the marginal likelihood can be obtained using a Gaussian prior distribution on the coefficients (Li and Clyde, 2018). This allows us to employ BMS-based approaches for estimation in GAMs with distributions belonging to the exponential family. The approximation idea has occasionally been used for BMS-based approaches (e.g., DiMatteo et al., 2001) and has been widely accepted in the literature on GAM estimation with Bayesian P-splines to facilitate the computation (Sabanés Bové et al., 2015; Wood, 2017; Gressani and Lambert,

2021).

Using the Laplace approximation for BMS-based GAM estimation helps easily obtain a closed-form expression of the marginal likelihood with a Gaussian or Gaussian mixture prior for the coefficients. However, it remains unclear which prior distribution is best for our purpose of basis determination. In the literature on variable selection, it has been continually reported that mixture priors outperform the classical Gaussian prior called Zellner’s g-prior and its variants (Liang et al., 2008; Li and Clyde, 2018). Such mixture priors, also known as mixtures of g-priors, have many desirable properties and resolve the paradoxes of the g-prior (Liang et al., 2008). Various mixtures of g-priors have been proposed under the framework of linear regression (e.g., Zellner and Siow, 1980; Cui and George, 2008; Liang et al., 2008; Maruyama and George, 2011; Bayarri et al., 2012; Ley and Steel, 2012; Womack et al., 2014), and there have been a few attempts to extend them for the GLM (Sabanés Bové and Held, 2011; Held et al., 2015; Fouskakis et al., 2018). Recently, Li and Clyde (2018) unified and extended mixtures of g-priors for the GLM using truncated compound confluent hypergeometric distributions (Gordy, 1998b), which encompass the currently existing mixture prior distributions. Still, the mixture prior that performs the best for BMS-based GAM estimation remains unknown. To resolve this, one must understand how mixtures of g-priors behave to penalize the nonparametric functions. The best mixture prior for nonparametric regression is unclear even for Gaussian additive regression.

Another important part of prior specification for BMS-based methods is a prior distribution on a set of intrinsic basis terms. Given that spline basis functions are often fully determined by knot locations, this is naturally translated into a prior on knots. Many prior distributions have been proposed to strike a balance between computational convenience and estimation quality (e.g., Smith and Kohn, 1996; Denison et al., 1998a; DiMatteo et al., 2001; Shen and Ghosal, 2015). The existing prior distributions on knots may be grouped into a few classes based on the doctrine of their constructions; the more flexible the prior, the better the approximation, but the greater the computational burden. Unfortunately, it has remained unclear which class of prior distributions is best for determining the best knots for splines from a practical point of view.

The contributions of this study are three-fold. First, we methodize the BMS-based approaches for GAM estimation using the Laplace approximation and unified framework of mixtures of g-priors systematized by Li and Clyde (2018). Compared with other variants of the g-prior for the exponential family models, the prior constructed in Li and Clyde (2018) has a few computational and structural advantages. To facilitate the computation, we propose a form of natural cubic spline functions suited for the BMS-based approaches. An R package that implements the sampling algorithms for our GAM estimation is available on the first author’s GitHub.¹ Second, among the various mixtures of g-priors belonging to a general class, we provide a default mixture prior for GAM estimation. To this end, an understanding of mixtures of g-priors is provided as a penalty to the model in order to see how mixture priors behave while estimating GAMs. The empirical performance of mixture priors is also investigated through an extensive simulation study. Our experience indicates that a traditional g-prior directly utilizing the sample size, also known as the unit information prior (Kass and Wasserman, 1995), may not be suitable and a mixture of g-priors should be used instead. Lastly, we categorize the prior distributions for knots

¹<https://github.com/hun-learning94/gambms>

available in the literature into three groups and examine which class is the best for estimation of GAMs. Our investigation shows that a prior distribution that is well-balanced between flexibility and accessibility performs the best; in other words, the most flexible prior, coined as the free-knot spline (Denison et al., 1998a; DiMatteo et al., 2001), is an overkill for GAM estimation in practice, whereas a less flexible but computationally friendly approach based on variable selection (Smith and Kohn, 1996) shows successful empirical results with fast mixing. We support our claims in this study with a verity of numerical results.

The remainder of this paper is structured as follows. Section 2 introduces the basic construction of GAMs using a spline basis expansion with natural cubic splines. Section 3 describes mixtures of g-priors for BMS under a unified framework, and compares the mixture priors for estimation of GAMs by interpreting them as penalty functions for nonparametric regression. In Section 4, we categorize the available prior distributions on knots into three different strategies for the BMS-based approaches. In Section 5, comprehensive simulation and numerical studies are performed to determine the best prior distribution and to compare the BMS-based approaches with their Bayesian competitors for GAM estimation. Lastly, Section 6 concludes the study with a discussion. The supplementary material includes proofs of the propositions, an additional simulation study, analysis of a real dataset, and a description for the installation of our R package.

2 Generalized additive models via basis expansion

For given predictor variables $x_i = (x_{i1}, x_{i2}, \dots, x_{ip})^T \in \mathbb{R}^p$, suppose that a response variable $Y_i \in \mathbb{R}$ has a distribution belonging to the exponential family of distributions; that is, the density of Y_i is

$$p(Y_i; \theta_i, \phi) = \exp \left(\frac{Y_i \theta_i - b(\theta_i)}{\phi} + c(Y_i, \phi) \right), \quad i = 1, \dots, n, \quad (1)$$

where θ_i is a natural parameter modeled by x_i , ϕ is a scale parameter, and b and c are known functions. The dependency of θ_i on x_i is clarified below. We mainly focus on the case in which the dispersion parameter ϕ is known; however, we also consider Gaussian regression with unknown ϕ in the supplementary material. Assuming that b is twice differentiable and $b''(\theta_i) > 0$, the expected value and variance of Y_i are given by $E(Y_i) = b'(\theta_i)$ and $Var(Y_i) = \phi b''(\theta_i)$, respectively. We choose a monotonically increasing link function h that parameterizes the natural parameter as $\theta_i = (h \circ b')^{-1}(\eta_i)$, where η_i is an additive predictor expressed as

$$\eta_i = \alpha + \sum_{j=1}^p f_j(x_{ij}), \quad i = 1, \dots, n, \quad (2)$$

with a global mean parameter α and univariate functions $f_j : \mathbb{R} \rightarrow \mathbb{R}$, $j = 1, \dots, p$. To ensure the identifiability, the functions f_j are assumed to satisfy $\sum_{i=1}^n f_j(x_{ij}) = 0$, $j = 1, \dots, p$.

In the complete model specification, the most important part is determining how to characterize the nonparametric functions f_j . Throughout this study, the functions f_j are parameterized using spline basis representation. Therefore, f_j are expressed as linear combinations of K_j basis

functions b_{j1}, \dots, b_{jK_j} ; that is, with coefficients $\beta_{jk} \in \mathbb{R}$,

$$f_j(\cdot) = \sum_{k=1}^{K_j} \beta_{jk} b_{jk}(\cdot), \quad j = 1, \dots, p.$$

For the identifiability condition $\sum_{i=1}^n f_j(x_{ij}) = 0$ to be satisfied, we assume that each basis function satisfies $\sum_{i=1}^n b_{jk}(x_{ij}) = 0$, $j = 1, \dots, p$. This can be easily achieved by centering an unrestricted basis term b_{jk}^* as

$$b_{jk}(\cdot) = b_{jk}^*(\cdot) - \frac{1}{n} \sum_{i=1}^n b_{jk}^*(x_{ij}), \quad j = 1, \dots, p, \quad k = 1, \dots, K_j. \quad (3)$$

Let $B_j \in \mathbb{R}^{n \times K_j}$ be a matrix whose (i, k) th component is $b_{jk}(x_{ij})$. The centering procedure is easily achieved by the projection $B_j = (I_n - n^{-1} \mathbf{1}_n \mathbf{1}_n^T) B_j^*$ with an unrestricted basis matrix B_j^* defined with b_{jk}^* for its (i, k) th component. We define a matrix $B = [B_1, \dots, B_p] \in \mathbb{R}^{n \times J}$ and a global vector of coefficients $\beta = (\beta_{11}, \dots, \beta_{1K_1}, \dots, \beta_{p1}, \dots, \beta_{pK_p})^T \in \mathbb{R}^J$, where $J = \sum_{j=1}^p K_j$. We then write a vector of additive predictors $\eta = (\eta_1, \dots, \eta_n)^T$ as $\eta = \alpha \mathbf{1}_n + B\beta$.

Many classes of basis functions can be used for smooth function estimation, such as B-splines (De Boor, 1978), wavelets (Antoniadis, 1997), radial basis functions (Buhmann, 2003), and Fourier basis functions (Katznelson, 2004). In this study, we deploy natural cubic spline basis functions to prevent erratic behavior at the boundaries. This is equivalent to using any type of piecewise polynomial basis functions (including B-splines) with suitable natural boundary conditions, provided that a prior distribution is invariant to the linear transformations of a design matrix (more precisely, invariant to isomorphisms). Specifically, for boundary knots $\{t^L, t^U\}$ and the set of M interior knots $\{t_1, \dots, t_M\}$ satisfying $-\infty < t^L < t_1 < \dots < t_M < t^U < \infty$, we define natural cubic spline basis functions $N_k : \mathbb{R} \rightarrow \mathbb{R}$, $k = 1, \dots, M+1$, as

$$\begin{aligned} N_1(u) &= u, \\ N_{k+1}(u) &= N(u; t^L, t^U, t_k) \\ &\equiv \frac{(u - t_k)_+^3 - (u - t^U)_+^3}{t^U - t_k} - \frac{(u - t^L)_+^3 - (u - t^U)_+^3}{t^U - t^L}, \quad k = 1, \dots, M. \end{aligned} \quad (4)$$

Along with the constant term $N_0(u) = 1$, the basis functions in (4) generate piecewise cubic functions. These functions are restricted as linear beyond the boundary knots $\{t^L, t^U\}$, resulting in increased stability near the boundaries caused by the induced constraints at $\{t^L, t^U\}$. The constant term is excluded in (4) because it is redundant given the intercept term. Compared with cubic splines without natural conditions, our experience shows (as is well known) that the use of natural cubic splines substantially reduces estimation bias near the boundaries.

Although the basis construction in (4) is based on the truncated power series, our definition is slightly different from the form of truncated power natural cubic splines commonly used in the literature, for example, equations (5.4) and (5.5) in Hastie et al. (2009). It can be shown that the basis terms in (4) span the identical piecewise cubic polynomial space with natural boundary conditions. However, our definition in (4) has an additional nice property where inserting a new knot-point $t_* \in (t^L, t^U)$ simply leads to adding a new basis term defined as $N(\cdot; t^L, t^U, t_*)$ into the

set $\mathcal{N} = \{N_k, k = 0, 1, \dots, M + 1\}$ without altering the current basis terms in \mathcal{N} . This property may not be present in other natural cubic spline basis functions, such as the natural cubic B-spline basis and the basis in equations (5.4) and (5.5) of [Hastie et al. \(2009\)](#). This is because a single basis term may depend on more than two knots and inserting a knot-point may alter other basis terms. This fact makes our basis terms in (4) far more attractive for model selection-based approaches (see Sections 4.2 and 4.3). To our knowledge, this study is the first to utilize the form of natural cubic splines in (4). The properties are formalized in the following propositions.

Proposition 1. *The set \mathcal{N} is a basis for the cubic spline space with natural boundary conditions.*

Proposition 2. *The addition of a new interior knot-point $t_* \in (t^L, t^U)$ introduces a corresponding basis term $N(\cdot; t^L, t^U, t_*)$ into \mathcal{N} . Similarly, the elimination of an existing interior knot-point $t_k \in t$ eliminates a corresponding basis term $N(\cdot; t^L, t^U, t_k)$ in \mathcal{N} .*

Proofs of Propositions 1 and 2 are provided in the supplementary material. We choose our basis terms b_{jk}^* using the natural cubic spline basis functions in (4). Specifically, using the observed design points, we set the boundary knots as $\xi_j^L = \min_{1 \leq i \leq n} x_{ij}$ and $\xi_j^U = \max_{1 \leq i \leq n} x_{ij}$ for each j . Then, with a given set of knots $\xi_j = \{\xi_{j1}, \dots, \xi_{jL_j}\}$ satisfying $\xi_j^L < \xi_{j1} < \dots < \xi_{jL_j} < \xi_j^U$, the unrestricted basis terms are chosen as

$$b_{j1}^*(\cdot) = N_1(\cdot), \quad b_{j,k+1}^*(\cdot) = N(\cdot; \xi_j^L, \xi_j^U, \xi_{jk}), \quad k = 1, \dots, L_j. \quad (5)$$

The class of spline functions is highly dependent on the specification of knots $\xi = \{\xi_1, \dots, \xi_p\}$. This, it is essential to choose a suitable knot placement to capture the local and global functional characteristics while avoiding overfitting. From the Bayesian point of view, a convenient approach is to let the data choose the most appropriate knots ξ from a predetermined set Ξ via BMS. The idea has become widely accepted in the literature (e.g., [Smith and Kohn, 1996](#); [Denison et al., 1998a](#); [DiMatteo et al., 2001](#); [Rivoirard and Rousseau, 2012](#); [De Jonge and Van Zanten, 2012](#); [Shen and Ghosal, 2015](#); [Jeong and Park, 2016](#); [Jeong et al., 2017](#)). A set Ξ can be a countable or uncountable collection of knots, that is, $\xi \in \Xi$. A richer Ξ provides flexible estimation for the regression spline functions, but may cause computational inefficiency. Under the Bayesian framework, specifying Ξ using a predetermined law can be viewed as assigning a prior distribution on ξ over the infinite-dimensional space for all possible knot locations with restricted support Ξ . The key to success is how to put a prior on ξ with a suitably restricted support Ξ . A few possibilities for a prior on ξ will be discussed in Section 4.

An additional advantage of the formulation in (5) is that the fully linear relationship is also easily characterized by our specification. More precisely, if ξ_j is empty, the basis consists only of the linear term b_{j1}^* . This situation is especially beneficial when a predictor variable is binary or assumed to have a linear effect. In this scenario, we may simply set the corresponding ξ_j to be an empty set, which is viewed as assigning a point mass prior to empty ξ_j . As a result, generalized additive partial linear models (GAPLMs), with both parametric and nonparametric additive terms ([Wang et al., 2011](#)), are naturally subsumed by our construction without any modifications.

One of the main advantages of BMS-based approaches to nonparametric regression is that they provide model-averaged estimates instead of resorting to a specific knot location. Our goal

is to examine model-averaged estimates of a functional $\mathcal{L} : (\alpha, f_1, \dots, f_p) \mapsto \mathcal{L}(\alpha, f_1, \dots, f_p)$ of interest, which is parameterized by the coefficients α and β . For example, we may be interested in a pointwise evaluation of the additive predictor $\alpha + \sum_{j=1}^p f_j(x_j)$ or the univariate functions $f_j(x_j)$, $j = 1, \dots, p$, at some $x = (x_1, \dots, x_p)^T$. The model-averaged posterior of a functional is given by

$$\pi(\mathcal{L}(\alpha, f_1, \dots, f_p) \mid Y) = \int_{\Xi} \pi(\mathcal{L}(\alpha, f_1, \dots, f_p) \mid \xi, Y) d\Pi(\xi \mid Y). \quad (6)$$

A key to our Bayesian procedure is how to assign a prior distribution for model selection and how the posterior distribution of ξ , $\Pi(\xi \mid Y)$, can be explored. In what follows, we write $B_\xi = B$, $\beta_\xi = \beta$, $J_\xi = J$, and $\eta_\xi = \alpha 1_n + B_\xi \beta_\xi$ to emphasize the dependency on ξ . Observe that $J_\xi = p + \sum_{j=1}^p |\xi_j|$, where $|\xi_j|$ is the number of knots ξ_j , $j = 1, \dots, p$.

3 Mixtures of g-priors for model selection-based estimation

Our main objective is to explore the posterior distribution of a functional $\mathcal{L}(\alpha, f_1, \dots, f_p)$. To obtain a model-averaged estimate, we need to (numerically) evaluate the integration in (6), which requires exploring the posterior distribution $\Pi(\alpha, \beta_\xi, \xi \mid Y)$. Accordingly, we need to specify a prior distribution $\Pi(\alpha, \beta_\xi, \xi)$ jointly over the parameter space. Possible priors for ξ , $\Pi(\xi)$, will be discussed in Section 4. The remaining crucial part is determining a prior for the knot-specific coefficients β_ξ , that is, $\Pi(\beta_\xi \mid \xi)$, for which this study employs mixtures of g-priors. Here we elucidate mixtures of g-priors for BMS-based approaches to GAMs and the resulting posteriors. We also provide a toy example to understand how the mixture priors penalize GAMs.

3.1 Mixtures of g-priors for exponential family models

We specify a prior distribution $\Pi(\alpha, \beta_\xi \mid \xi) = \Pi(\alpha)\Pi(\beta_\xi \mid \xi)$. Following the convention, we assign an improper uniform prior on the common parameter α , that is,

$$\pi(\alpha) \propto 1. \quad (7)$$

The use of this improper prior has been justified in the literature (Berger et al., 1998; Bayarri et al., 2012). Next, we discuss $\Pi(\beta_\xi \mid \xi)$. For model selection in linear regression, Zellner's g-prior is often preferred because of its computational efficiency and invariance to linear transformations (Zellner, 1986). In our spline setup, invariance to transformations of a design matrix is particularly appealing because it is ideal if the procedure is invariant to a specific choice of basis functions, as long as a target spline space is correctly generated. Therefore, this invariance of the g-prior supports our spline basis system defined in (5) because of Proposition 1. Unfortunately, the computational advantage of the g-prior is generally lost in GAMs because normal priors are not conjugate to non-normal likelihoods, resulting in the inability to achieve a closed-form expression of the marginal likelihood $p(Y \mid \xi)$. The computation for the posterior distribution in (6) becomes more challenging without the calculation of the marginal likelihood. Therefore, we consider approximating the marginal likelihood using the Laplace approximation with a suitable variant of the g-prior. The Laplace approximation has occasionally been used for nonparametric regression with g-priors (e.g., DiMatteo et al., 2001).

For the function $\theta = (h \circ b')^{-1}$, let $J_n(\hat{\eta}_\xi) = \text{diag}(-Y_i \theta''(\hat{\eta}_{\xi,i}) + (b \circ \theta)''(\hat{\eta}_{\xi,i}), i = 1, \dots, n)$ be the observed information matrix of η_ξ evaluated at $\hat{\eta}_\xi$ (defined as the Hessian matrix of the negative log-likelihood), where $\hat{\eta}_\xi = (\hat{\eta}_{\xi,1}, \dots, \hat{\eta}_{\xi,n})^T = \hat{\alpha}_\xi \mathbf{1}_n + B_\xi \hat{\beta}_\xi$ with the maximum likelihood estimators $\hat{\alpha}_\xi$ and $\hat{\beta}_\xi$ (assuming that $\hat{\alpha}_\xi$ and $\hat{\beta}_\xi$ exist). We restrict our attention to the case where $J_n(\hat{\eta}_\xi)$ is positive definite. This is usually the case except for a few extreme situations such as the complete separation in logistic regression (Li and Clyde, 2018). In this study, we deploy the following variant of the g-prior proposed by Li and Clyde (2018),

$$\beta_\xi \mid g, \xi \sim N(0, g(\tilde{B}_\xi^T J_n(\hat{\eta}_\xi) \tilde{B}_\xi)^{-1}), \quad (8)$$

where $\tilde{B}_\xi = [I_n - \text{tr}(J_n(\hat{\eta}_\xi))^{-1} \mathbf{1}_n \mathbf{1}_n^T J_n(\hat{\eta}_\xi)] B_\xi$ is the matrix consisting of the columns of B_ξ centered by the weighted average with the diagonal elements of $J_n(\hat{\eta}_\xi)$. The prior in (8) requires $\tilde{B}_\xi^T J_n(\hat{\eta}_\xi) \tilde{B}_\xi$ to be invertible. This is satisfied if and only if B_ξ is of full-column rank (observe that $J_n(\hat{\eta}_\xi)$ is positive definite and $\text{rank}(B_\xi) = \text{rank}(\tilde{B}_\xi)$). Hence, the full-column rank condition will be made for $\Pi(\xi)$ in Section 4. Although the prior in (8) can be extended by adopting a generalized inverse, we do not pursue this direction. We refer the reader to Section 2.5 of Li and Clyde (2018) for further discussion on when B_ξ is not of full-column rank.

In addition to the prior in (8), there exist many other variants of the g-prior for the exponential family models (e.g., Kass and Wasserman, 1995; Hansen and Yu, 2003; Gupta and Ibrahim, 2009; Sabanés Bové and Held, 2011; Held et al., 2015). Here we adopt the prior in (8) because it provides a convenient expression for the approximate marginal likelihood. Moreover, our prior may better capture the large sample covariance structures and local geometry than other variants of the g-prior (Li and Clyde, 2018). It is worth mentioning that the prior in (8) is dependent on the observation vector Y , which shows it should be accepted by the empirical Bayes philosophy. Nonetheless, we suppress the dependency on Y in the expression of (8) for notational convenience.

Integrating the second order Taylor expansion for the likelihood with respect to (7) and (8), we obtain

$$p(Y \mid g, \xi) = p(Y \mid \hat{\eta}_\xi) \text{tr}(J_n(\hat{\eta}_\xi))^{-1/2} (g+1)^{-J_\xi/2} \exp\left(-\frac{Q_\xi}{2(g+1)}\right), \quad (9)$$

where $p(Y \mid \hat{\eta}_\xi)$ is the likelihood evaluated at $\hat{\eta}_\xi$ with given ξ and $Q_\xi = \hat{\beta}_\xi^T \tilde{B}_\xi^T J_n(\hat{\eta}_\xi) \tilde{B}_\xi \hat{\beta}_\xi$ is the Wald statistic. The expression in (9) shows that if g is predetermined as a hyperparameter, the marginal likelihood is highly sensitive to its specification. A suitable value for g has been extensively debated in the literature. The most common choice is letting $g = n$, called the unit information prior (Kass and Wasserman, 1995). This idea has also been widely adopted in the literature on nonparametric regression using BMS (e.g. Gustafson, 2000; DiMatteo et al., 2001; Kohn et al., 2001). From the Bayesian perspective, the unit information prior can be viewed as a point mass prior at $g = n$, that is, $\Pi(g) = \delta_n(g)$ with the Dirac measure δ_b at b . However, it has been reported that putting a suitable prior distribution on g , called a mixture of g-priors, leads to improved empirical performance while addressing the paradoxes in BMS (Liang et al., 2008; Li and Clyde, 2018). To unify various mixtures of g-priors, we use a broad family that encompasses various mixture distributions. Specifically, following Li and Clyde (2018), we assign the truncated

	a	b	r	s	ν	κ	Concentration
Uniform	2	2	0	0	1	1	$g = O(1)$
Hyper- g	1	2	0	0	1	1	$g = O(1)$
Hyper- g/n	1	2	1.5	0	1	n^{-1}	$g = O(n)$
Beta-prime	0.5	$n - J_\xi - 1.5$	0	0	1	1	$g = O(n)$
ZS-adapted	1	2	0	$n + 3$	1	1	$g = O(n)$
Robust	1	2	1.5	0	$\frac{n+1}{J_\xi+1}$	1	$g = O(n)$
Intrinsic	1	1	1	0	$\frac{n+J_\xi+1}{J_\xi+1}$	$\frac{n+J_\xi+1}{n}$	$g = O(n)$

Table 1: Distributions belonging to the tCCH family.

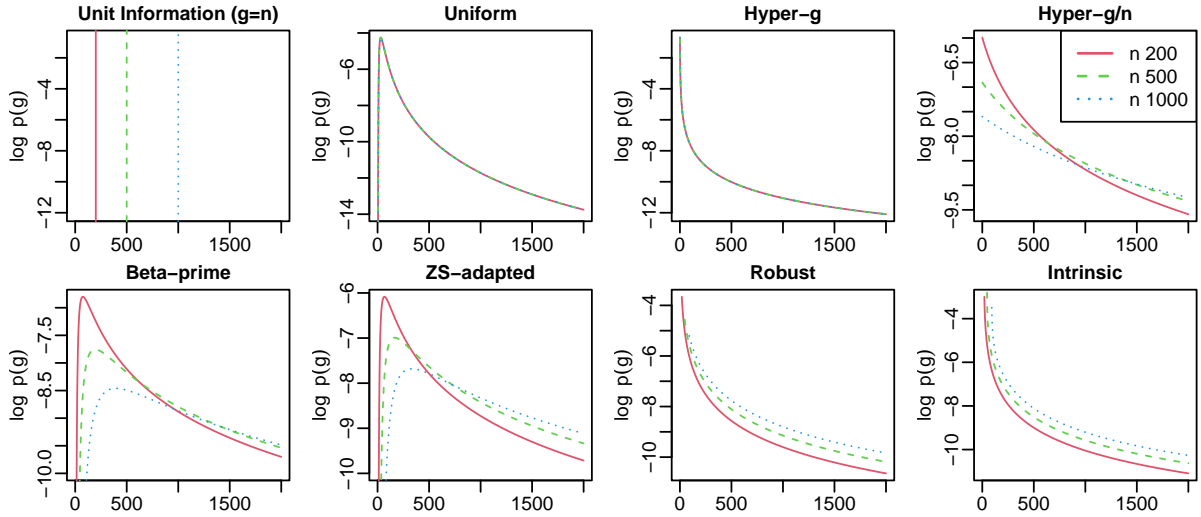


Figure 1: Distributions belonging to the tCCH family for $n = 200, 500, 1000$, with $J_\xi = 10$ if required.

compound confluent hypergeometric (tCCH) distribution to $(g + 1)^{-1}$ (Gordy, 1998b), that is,

$$\frac{1}{g+1} \sim \text{tCCH}\left(\frac{a}{2}, \frac{b}{2}, r, \frac{s}{2}, \nu, \kappa\right), \quad a, b, \kappa > 0, \quad r, s \in \mathbb{R}, \quad \nu \geq 1. \quad (10)$$

See (18) in the supplementary material to examine the density of the tCCH distribution.

Table 1 shows a few distributions belonging to the tCCH family: the uniform prior (on $(g + 1)^{-1}$), the hyper- g and hyper- g/n priors (Liang et al., 2008), beta-prime prior (Maruyama and George, 2011), Zellner Siow (ZS)-adapted prior (Held et al., 2015), robust prior (Bayarri et al., 2012), and intrinsic prior (Womack et al., 2014). The beta-prime prior is proper only if $J_\xi < n - 1$, so this restriction needs to be incorporated in $\Pi(\xi)$ if the beta-prime prior is used. According to Li and Clyde (2018), the prior distributions are classified into two groups based to the prior concentration: $g = O(1)$ and $g = O(n)$. (Notation can be misleading; it refers to the order of concentration of the distribution rather than the value of g . Maruyama and George (2011) also uses the same notation.) Figure 1 illustrates how the concentration of each prior distribution on g behaves.

The resulting marginal likelihood is expressed as

$$p(Y | \xi) = p(Y | \hat{\eta}_\xi) \text{tr}(J_n(\hat{\eta}_\xi))^{-1/2} \nu^{-J_\xi/2} \exp\left(-\frac{Q_\xi}{2\nu}\right) \frac{B((a + J_\xi)/2, b/2)}{B(a/2, b/2)} \times \Phi_1\left(\frac{b}{2}, r, \frac{a + b + J_\xi}{2}, \frac{s + Q_\xi}{2\nu}, 1 - \kappa\right) \Big/ \Phi_1\left(\frac{b}{2}, r, \frac{a + b}{2}, \frac{s}{2\nu}, 1 - \kappa\right), \quad (11)$$

where $B(\cdot, \cdot)$ is the beta function and $\Phi_1(\alpha, \beta, \gamma, x, y) = B(\alpha, \gamma - \alpha)^{-1} \int_0^1 u^{\alpha-1} (1-u)^{\gamma-\alpha-1} (1-yu)^{-\beta} e^{xu} du$ is the confluent hypergeometric function of two variables (Humbert, 1922). Generally, the evaluation of Φ_1 cannot be analytically performed and has to rely on numerical approximation. To calculate Φ_1 , we use the Gaussian-Kronrod quadrature routine available in the Boost C++ library.

It is not difficult to show that the approximate posterior for $((g+1)^{-1}, \alpha, \beta_\xi)$ conditional on ξ is given by

$$\begin{aligned} \frac{1}{g+1} | Y, \xi &\sim \text{tCCH}\left(\frac{a + J_\xi}{2}, \frac{b}{2}, r, \frac{s + Q_\xi}{2}, \nu, \kappa\right), \\ \alpha | Y, g, \xi &\sim N(\hat{\alpha}_\xi, \text{tr}(J_n(\hat{\eta}_\xi))^{-1}), \\ \beta_\xi | Y, g, \xi &\sim N\left(\frac{g}{g+1} \hat{\beta}_\xi, \frac{g}{g+1} (\tilde{B}_\xi^T J(\hat{\eta}_\xi) \tilde{B}_\xi)^{-1}\right). \end{aligned} \quad (12)$$

The expression is also valid for the unit information prior by replacing the first line with the point mass posterior, that is, $\Pi(g | Y, \xi) = \delta_n(g)$. Sampling from tCCH distributions can be carried out through MCMC, but exact sampling is available under some prior specification. We observe that if any of the uniform prior, hyper-g prior, ZS-adapted prior, or robust prior is used, the first line of (12) is reduced to a truncated gamma distribution and exact sampling is straightforward (see Section B in the supplementary material). The joint posterior $\Pi(\alpha, \beta_\xi, \xi, g | Y)$ is fully specified with the posterior in (12) and the marginal posterior of ξ , that is, $\Pi(\xi | Y)$. The latter one is obtained by specifying a prior $\Pi(\xi)$ as in Section 4 and deploying the expression for the approximate marginal likelihood $p(Y | \xi)$ in (11) (or $p(Y | g, \xi)$ in (9) for the unit information prior). Then the posterior distribution of a functional in (6) is easily evaluated by directly marginalizing ξ out or using MCMC for Monte Carlo integration for ξ , depending on a prior for ξ specified in Section 4.

3.2 Complexity penalty by mixtures of g-priors

The influence of g is crucial for reasonable sparsity in model selection with the g-prior (Kass and Raftery, 1995); a large g favors sparse models, while a small g advocates complex models. In particular, choosing a suitable g is extremely important in our additive model setup because it directly controls the smoothness of the additive functions. In the literature on nonparametric regression with basis expansion, many previous studies have relied on the unit information prior induced by the choice $g = n$ (e.g. Gustafson, 2000; DiMatteo et al., 2001; Kohn et al., 2001). However, as noted before, a mixture of g-priors leads to improved empirical performance in BMS (Liang et al., 2008; Li and Clyde, 2018). There have been attempts to put a prior on g for nonparametric regression (Jeong and Park, 2016; Jeong et al., 2017; Francom et al., 2018; Park

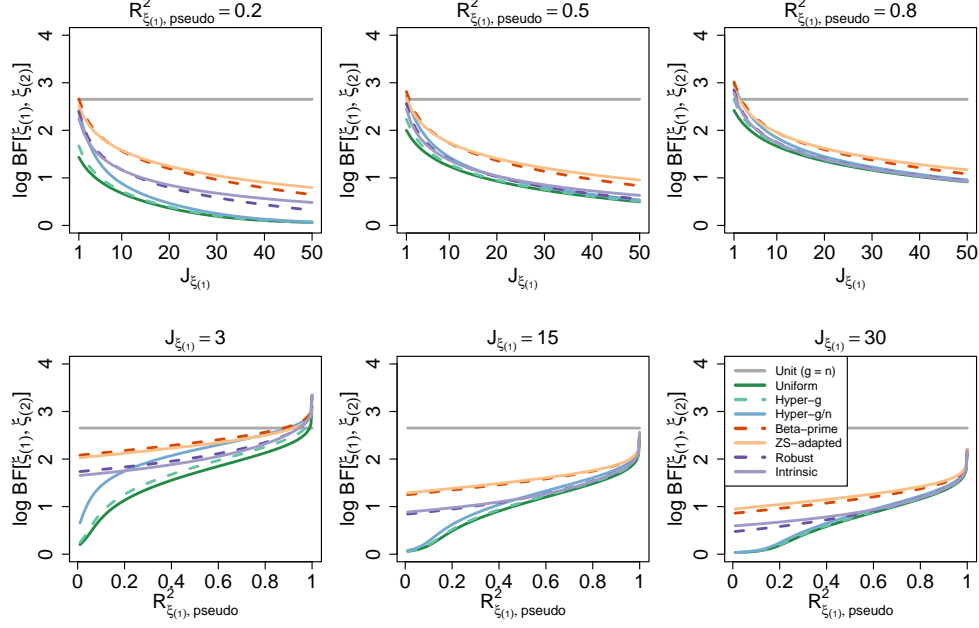


Figure 2: The log Bayes factor $\log BF[\xi_{(1)}; \xi_{(2)}]$ as a function of $J_{\xi_{(1)}} (= J_{\xi_{(2)}} + 1)$ and the goodness-of-fit measurement for $n = 1000$.

and Jeong, 2018; Francom and Sansó, 2020; Jeong et al., 2022), but a thorough investigation into how the priors differ from the unit information prior is lacking. In this section, we examine how the behavior of mixtures of g-priors differs from that of the unit information prior with $g = n$ and why the unit information prior may not be a good choice for estimation of GAMs.

Our investigation is based on the Bayes factors. For two knots $\xi_{(1)}$ and $\xi_{(2)}$, the Bayes factor of $\xi_{(1)}$ to $\xi_{(2)}$ is defined as $BF[\xi_{(1)}; \xi_{(2)}] = p(Y | \xi_{(1)})/p(Y | \xi_{(2)})$. For the exponential family models with known ϕ , the marginal likelihood $p(Y | \xi)$ is expressed by (9) with $g = n$ for the unit information prior and (11) for mixtures of g-priors induced by the tCCH prior on $(g + 1)^{-1}$.

To understand how the Bayes factor penalizes model complexity, we consider two knots $\xi_{(1)}$ and $\xi_{(2)}$ such that $J_{\xi_{(1)}} = J_{\xi_{(2)}} + 1$ and $\hat{\eta}_{\xi_{(1)}} = \hat{\eta}_{\xi_{(2)}}$. Thus, the two knots equally contribute to model fit but $\xi_{(1)}$ has one more redundant knot-point than $\xi_{(2)}$. The Bayes factor $BF[\xi_{(1)}; \xi_{(2)}]$ can be interpreted as a penalty against the more complex model with one more redundant knot-point; the larger the value of the log Bayes factor, the stronger the penalty on the larger model. We see how the Bayes factor behaves as $J_{\xi_{(1)}}$ and the goodness-of-fit change. For Gaussian regression, the goodness-of-fit can be naturally measured by the coefficient of determination. For the exponential family models, the pseudo- R^2 , defined as $1 - \exp(-D/n)$ with the usual deviance statistic D , can instead be used (Cox and Snell, 1989; Magee, 1990), albeit with the caveat where the maximum value may be less than 1 depending on the specific model (Nagelkerke, 1991). To express the Bayes factor as a function of the pseudo- R^2 , we use the fact that Q_ξ is asymptotically equivalent to the deviance D under mild conditions (Held et al., 2015; Li and Clyde, 2018). Therefore, we define $R^2_{\xi, \text{pseudo}} = 1 - \exp(-Q_\xi/n)$ to measure the goodness-of-fit in the exponential family models.

Figure 2 visualizes a toy example with $n = 1000$, which shows how the log Bayes factor

$\log BF[\xi_{(1)}; \xi_{(2)}]$ behaves as $J_{\xi_{(1)}}$ (which equals $J_{\xi_{(2)}} + 1$) and $R_{\xi_{(1)}, \text{pseudo}}^2$ (which equals $R_{\xi_{(2)}, \text{pseudo}}^2$) change. It is clear that the unit information prior always yields a constant penalty regardless of $J_{\xi_{(1)}}$ and the goodness-of-fit. On the other hand, the first row of Figure 2 illustrates that the penalty functions produced by the mixture priors get weaker as the model size $J_{\xi_{(1)}}$ increases. This indicates that, when small models are compared, mixtures of g-priors favor the sparser model ($\xi_{(2)}$) unless there is a significant improvement in the marginal likelihood. In contrast, when large models are compared, the mixture priors advocate the more complex model ($\xi_{(1)}$) even if the gain is not sufficiently clear. This property can be useful in improving the performance in GAM estimation because the basis expansion produces a large model in general and we wish to detect local and global signals of the target functions that may be easily missed. The second row of Figure 2 shows that the penalty functions induced by the mixture priors become stronger as the goodness-of-fit measurement increases. This is in accordance with the intuition because if the goodness-of-fit is good enough, we may not want to opt for the more complex model and instead choose the sparser one, unless the complex model significantly improves the marginal likelihood.

The behavior of the log Bayes factor illustrated in Figure 2 indicates that the unit information prior may not be a suitable choice for estimation of GAMs, and the mixtures of g-priors can be an alternative. However, it remains unclear which mixture prior would perform the best for GAMs. Figure 2 also demonstrates the differences among the mixtures of g-priors. The beta-prime and ZS-adapted priors behave similarly and exhibit the strongest penalties among the candidates. The robust and intrinsic priors show similar decays to each other and are weaker than the beta-prime and ZS-adapted priors. The two $O(1)$ -type priors (uniform and hyper-g) yield the weakest penalties and are weaker than other $O(n)$ -type priors. The hyper-g/n prior is somewhat special and appears to be close to the $O(1)$ -type priors, even though it belongs to the $O(n)$ family. Although the figure shows that the mixtures of g-priors behave differently, it hardly reveals the best mixture prior for GAMs. The answer to this question should be based on suitable simulation studies as provided in Section 5. The following proposition provides a basic interpretation of where such discrepancies may arise.

Proposition 3. *For the model in (1) and (2) with the prior in (8), consider two knots $\xi_{(1)}$ and $\xi_{(2)}$ such that $J_{\xi_{(1)}} = J_{\xi_{(2)}} + k$ and $\hat{\eta}_{\xi_{(1)}} = \hat{\eta}_{\xi_{(2)}}$, where k is a positive integer. Then, for any positive integer k ,*

$$BF[\xi_{(1)}; \xi_{(2)}] = \begin{cases} (1+b)^{-k/2}, & \text{if } g \sim \delta_b, \\ E[(1+g)^{-k/2} \mid \xi_{(2)}, Y], & \text{if } g \sim tCCH(a/2, b/2, r, s/2, \nu, \kappa). \end{cases}$$

A proof of Proposition 3 is provided in the supplementary material. Proposition 3 implies that the Bayes factor $BF[\xi_{(1)}; \xi_{(2)}]$ is the conditional posterior mean of $(1+g)^{-k/2}$ induced by the unit information or tCCH priors. Hence, the proposition explicitly shows why the penalty function induced by the unit information prior is constant. The differences in the penalties induced by the mixture priors can be attributed to different posterior means of the shrinkage factor $(1+g)^{-k/2}$.

As a final note, coupled with a specified prior for knots $\Pi(\xi)$, the actual model comparison for the determination of basis terms is based on the posterior odds $\Pi(\xi_{(1)} \mid Y)/\Pi(\xi_{(2)} \mid Y)$ instead of the Bayes factor. Thus, one might want to adjust the posterior odds induced by the unit

information prior using a suitable prior for knots $\Pi(\xi)$ such that it behaves like the mixtures of g-priors as in Figure 2. Although this is not entirely impossible, a prior for knots must be highly data-dependent in order for the posterior odds with the unit information prior to adapt to the goodness-of-fit measurement. Therefore, using the mixtures of g-priors with a usual prior for knots is much more natural.

4 Priors for knots

A prior $\Pi(\alpha, \beta_\xi \mid \xi)$ on the coefficients was specified in Section 3. To complete the Bayesian framework, here we consider a few different options for specifying $\Pi(\xi)$ for knots. We observed that our prior for β_ξ requires B_ξ to be of full-column rank (see (8) above). Therefore, we choose $\Pi(\xi)$ with the condition that B_ξ is of full-column rank with prior probability one, that is, $\Pi(\text{rank}(B_\xi) = J_\xi) = 1$. This is often fulfilled by the restriction $J_\xi < n$ if the knots and design points are well-distributed; nevertheless, we keep the general expression.

Intuitively, ξ_j can consist of any singletons lying on the interval (ξ_j^L, ξ_j^U) , indicating that the intrinsic parameter space for ξ_j is infinite-dimensional. However, finite truncation to restricted support may be helpful for computational reasons. As mentioned earlier, we denote Ξ as the induced support of a prior on ξ . The support Ξ restricts the function class generated by our natural cubic spline basis terms. A smaller space reduces model complexity but may fail to capture local and global features of the target function. This means that the restricted support Ξ balances estimation quality and computational efficiency, and is crucial to choose a prior with suitable Ξ . There have been various ideas of specifying Ξ for $\Pi(\xi)$. In this section, we gather the existing strategies for constructing Ξ that have been widely accepted in the literature and classify them into three categories. The three approaches are described in detail in Sections 4.1–4.3. Figure 3 provides a graphical summary of the strategies. This section only provides a systematic organization of the prior distributions on ξ . A comparison among the empirical performances of the three approaches is performed in Section 5 based on a numerical study.

4.1 Even-knot splines: equidistant knots

The simplest but powerful Bayesian adaptation arises from the assumption that the number of knots is not fixed but their locations are determined by an intrinsic law. The idea has been extensively considered in the literature and has been empirically and theoretically successful (e.g., Rivoirard and Rousseau, 2012; De Jonge and Van Zanten, 2012; Shen and Ghosal, 2015). We refer to this approach as the *even-knot splines*. The name should be carefully understood because evenness may be assessed by the empirical measure rather than a geometric distance.

Specifically, a prior is assigned on the number $|\xi_j|$ of knots ξ_j for $j = 1, \dots, p$. The remaining specification on ξ is automatically completed by a given rule. For example, with a given number $|\xi_j|$, the knots ξ_j may be equally spaced or chosen based on the quantiles of $\tilde{X}_j = \{x_{ij}\}_{i \in \{1, \dots, n\}}$, where \tilde{X}_j is the set of unique values of the design points $x_{ij}, i = 1, \dots, n$. We prefer the latter for the stable implementation. It also guarantees full-column rank of B_ξ as soon as $J_\xi < n$, if there are no duplicates in $x_{ij}, i = 1, \dots, n$. For computational reasons, it is also useful to put a cap on each $|\xi_j|$ such that $|\xi_j| \leq M_j$ for a predetermined M_j , even though it is not necessary. The

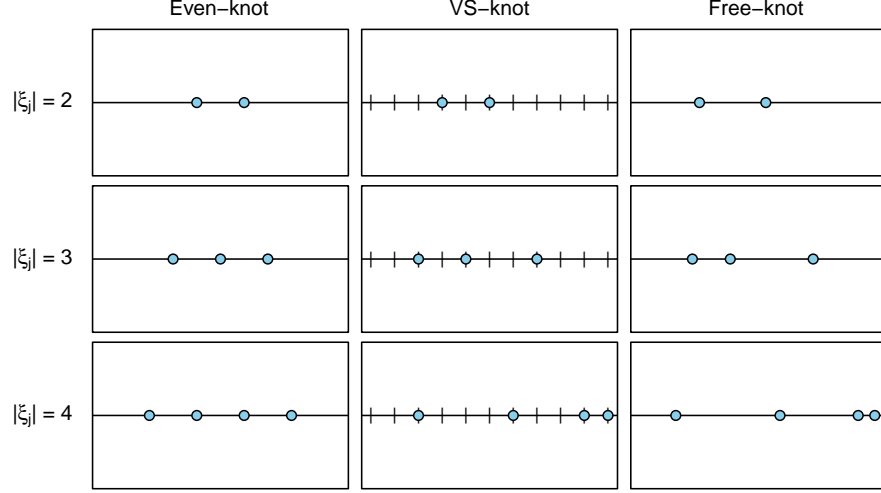


Figure 3: A graphical illustration of the three strategies for constructing Ξ discussed in Sections 4.1–4.3. For the even-knot splines, the locations of knots are deterministically ascertained once $|\xi_j|$ is chosen. The VS-knot splines select knot-points from a pre-determined set of locations. The free-knot splines are the most flexible and have no such limitation.

induced support is then defined as

$$\Xi_{EK} = \left\{ \xi : \text{rank}(B_\xi) = J_\xi, |\xi_j| \leq M_j, \xi_{jk} = Q_j\left(\frac{k}{|\xi_j|+1}\right), j = 1, \dots, p, k = 1, \dots, |\xi_j| \right\},$$

where Q_j is the quantile function of \tilde{X}_j , for $j = 1, \dots, p$. Examples of knots belonging to Ξ_{EK} are illustrated in Figure 3. With an unnormalized density function $q_j : \{0, 1, \dots, M_j\} \rightarrow (0, \infty)$ on $|\xi_j|$, the prior can be formally expressed as

$$\pi_{EK}(\xi) \propto \mathbb{1}(\text{rank}(B_\xi) = J_\xi) \prod_{j=1}^p q_j(|\xi_j|). \quad (13)$$

Further discussion on the density q_j will be provided in Section 4.4.

The key benefit of the prior in (13) is that it has low model complexity; that is, we can enumerate all possible models for moderately large p because $|\Xi_{EK}| \leq \prod_{j=1}^p (1 + M_j)$. This enables MCMC-free posterior computation for relatively low-dimensional problems. If p is too large to list all possibilities, the Metropolis-Hastings algorithm can be useful for exploring the model spaces with a proposal that increases or decreases $|\xi_j|$ at a time. In this situation, if p is moderately large, computation may be facilitated by saving the value of the marginal likelihood $p(Y | \xi)$ with current ξ and utilizing it whenever the same ξ is revisited. We observe that the storing idea works well unless p is too large.

Although the even-knot splines substantially reduce the model complexity, its major downside arises from its deterministic rule. Specifically, due to the nature of construction, it is impossible to deal with functions with spatially adaptive smoothness such as a Doppler function. This drawback motivates the need for more flexible constructions discussed in the next two subsections.

4.2 VS-knot splines: knot selection

The limitation of the even-knot splines in Section 4.1 can be relaxed by considering a prior inducing a richer Ξ that allows for spatial adaptation. This can be fulfilled by allowing knot placement as well as the number of knots to be data-driven. A common strategy is setting a large set of basis functions and choosing important ones among the candidates using Bayesian variable selection. The idea was initiated by Smith and Kohn (1996) and has been widely used in the literature on nonparametric regression (e.g., Kohn et al., 2001; Chan et al., 2006; Jeong and Park, 2016; Jeong et al., 2017; Park and Jeong, 2018; Jeong et al., 2022). Given that the approach is based on variable selection, we refer to it as the *VS-knot splines*.

Consider a set $\xi_j^c = \{\xi_{j1}^c, \dots, \xi_{jM_j}^c\}$ of knot candidates such that $\xi_j^L < \xi_{j1}^c < \dots < \xi_{jM_j}^c < \xi_j^U$ with large enough $M_j < n$. Similar to Section 4.1, ξ_j^c can be equidistant or determined by the sample quantiles of \tilde{X}_j . We prefer the latter setup. Then, the knots ξ_j are chosen as a subset of ξ_j^c (including an empty set) using BMS. Therefore, the support consists of all possible subsets of $\{\xi_1^c, \dots, \xi_p^c\}$ with the restriction $\text{rank}(B_\xi) = J_\xi$, i.e.,

$$\Xi_{VS} = \{\xi : \text{rank}(B_\xi) = J_\xi, \xi_j \subset \xi_j^c, j = 1, \dots, p\}.$$

Similar to Section 4.1, it is reasonable to assign an unnormalized density $q_j : \{0, 1, \dots, M_j\} \rightarrow (0, \infty)$ to $|\xi_j|$. And then we assign equal weights to all knot locations conditional on $|\xi_j|$. The resulting prior is given by

$$\pi_{VS}(\xi) \propto \mathbb{1}(\text{rank}(B_\xi) = J_\xi) \prod_{j=1}^p q_j(|\xi_j|) \binom{M_j}{|\xi_j|}^{-1}. \quad (14)$$

The prior has been shown to be successful in adapting to spatially inhomogeneous smoothness (e.g., Chan et al., 2006; Jeong and Park, 2016; Jeong et al., 2017). The cardinality $|\Xi_{VS}| \leq 2^{\sum_{j=1}^p M_j}$ shows that it is usually impractical to enumerate all possible models, indicating that MCMC is useful for exploring the model spaces. The standard Gibbs sampling and Metropolis-Hastings algorithm can be easily applied to this setup (Dellaportas et al., 2002). Sampling efficiency may be improved by block updates (Kohn et al., 2001; Jeong et al., 2022) or adaptive sampling (Nott and Kohn, 2005; Ji and Schmidler, 2013). Moreover, as Ξ_{VS} is finite-dimensional, the idea of storing the marginal likelihood discussed in Section 4.1 seems viable. However, our experience shows that this approach is effective only when p is very small because of the memory issue, for example, $p \leq 2$. Thus, we do not pursue this direction.

We emphasize that our basis system in (5) is particularly useful for the VS-spline approach. Given Proposition 2, knot selection is naturally translated into basis selection with the linear term b_{j1}^* always being included. This property makes the computation straightforward with the basis system in (4) and (5); one can generate a full basis matrix $B_j^c \in \mathbb{R}^{n \times (M_j+1)}$ whose (i, k) th component is $b_{jk}(x_{ij})$ constructed with the knot candidates $\xi_j^c = (\xi_{j1}^c, \dots, \xi_{jM_j}^c)$, and then choose important columns of B_j^c , while always including the first column for the linear term. As noted previously, this is not possible with other natural cubic spline basis functions, such as B-splines or the ones that are commonly used in the literature (Hastie et al., 2009). For these basis functions, a basis term $b_{j,k+1}^*$ is potentially specified with more than two knot-points for some k . Therefore, inserting or deleting a knot-point may alter more than two basis terms, leading to conflict between knot selection and basis selection.

4.3 Free-knot splines

The strategy of the VS-splines in Section 4.2 chooses important knot locations among a set of predetermined candidates. The resulting knots are not equally spaced so that they can account for spatially varying degree of smoothness. Despite this flexibility, there is a further desire to relax the restriction coming from the discrete set of knot candidates, with a fully nonparametric setup by allowing knots to be any singletons in the given range as soon as the induced B_ξ is of full-column rank. The idea is referred to as the *free-knot splines* (Denison et al., 1998a; DiMatteo et al., 2001).

Similar to Section 4.1, it can be useful to put a cap on each $|\xi_j|$ such that $|\xi_j| \leq M_j$ for a predetermined M_j . The resulting support for ξ is

$$\Xi_{FK} = \left\{ \xi : \text{rank}(B_\xi) = J_\xi, |\xi_j| \leq M_j, \xi_j^L < \xi_{j1} < \cdots < \xi_{j|\xi_j|} < \xi_j^U, j = 1, \dots, p \right\}.$$

It is clear that Ξ_{FK} is uncountable. The prior is specified in a manner similar to (14). However, as the map $|\xi_j| \mapsto \xi_j$ is a surjection and not a bijection, a conditional prior density of ξ_j given $|\xi_j|$, denoted by $\tilde{q}_j(\cdot \mid |\xi_j|)$, should be specified on the corresponding support. Following DiMatteo et al. (2001), we choose \tilde{q}_j induced by the uniform prior on the $|\xi_j|$ -simplex by scaling (ξ_j^L, ξ_j^U) to $(0, 1)$. With an unnormalized density $q_j : \{0, 1, \dots, M_j\} \rightarrow (0, \infty)$, the prior on ξ_j is formalized as

$$\pi_{FK}(\xi) \propto \mathbb{1}(\text{rank}(B_\xi) = J_\xi) \prod_{j=1}^p q_j(|\xi_j|) \tilde{q}_j(\xi_j \mid |\xi_j|). \quad (15)$$

Our free-knot spline prior in (15) is slightly more general than the original construction by DiMatteo et al. (2001) because at least one knot must be included in their construction, whereas we relaxed such limitation to account for a completely linear effect using an empty knot. The posterior distribution can be explored by the reversible jump MCMC with birth, death, and relocation proposals (DiMatteo et al., 2001). Thus, the computation is generally more demanding than the VS-knot splines. The accompanying benefit is that the prior is inherently more flexible than the one in (14) and has a better ability to approximate the target functions. However, our experience shows that there is no significant improvement in the free-knot splines in most practical examples. Considering that the reversible jump MCMC is often inefficient, this fact points out that the inadvertent use of the free-knot splines should be avoided. Our simulation study in Section 5 shows that, while the performance measures for the free-knot splines are comparable with those for the VS-knot splines, the sampling efficiency (measured as the ratio of the effective sample size and runtime) of the free-knot splines is significantly lower.

Similar to the VS-knot splines approach, the basis construction in (4) and (5) is useful for the free-knot splines. Given Proposition 2, adding or removing a knot-point corresponds to adding or removing the corresponding basis term. Hence, the reversible jump MCMC can be carried out by adding or removing a column of the matrix, without the need to reconstruct the entire basis terms.

4.4 More about the prior distribution on $|\xi_j|$

The priors described in Sections 4.1–4.3 require us to specify the unnormalized prior density q_j on $|\xi_j|$. Here, we discuss more about q_j . To achieve the desired optimal properties in nonparametric regression, it has been shown that priors for BMS-based methods must possess suitably decaying tail properties (e.g., [Shen and Ghosal, 2015](#)). Such priors with the guaranteed tail property include Poisson and geometric distributions (with a suitable truncation if required by the setup) ([Shen and Ghosal, 2015](#)). Although they enjoy the theoretical flavor, how to choose the practically right prior decay is unclear. In the literature on variable selection, another common choice (believed to be weakly informative) is a discrete uniform distribution on $\{0, 1, \dots, M_j\}$, resulting in the so-called hierarchical uniform prior on ξ_j ([Kohn et al., 2001](#); [Cripps et al., 2005](#); [Scott and Berger, 2010](#)). To maintain the balance between the theoretical flavor in nonparametric regression and practical grounds of model selection, we set our default prior to be a truncated geometric distribution with small success probability ϖ ; that is, the unnormalized density is

$$q_j(u) = (1 - \varpi)^u \varpi, \quad u = 0, 1, \dots, M_j. \quad (16)$$

With sufficiently small ϖ , the prior in (16) mimics the discrete uniform distribution, while preserving the desired tail property for the optimality.

The unnormalized density q_j can also be specified in a different manner to reduce the model complexity. As noted in Section 2, our model formulation subsumes GAPLMs, where a few predictor variables are assumed to have linear effect (e.g., binary variables). Because this restriction is implemented by fixing some f_j to be composed only based on the linear basis term N_1 , we can choose a point mass at zero as q_j for such j , i.e., $\Pi(|\xi_j| = 0) = 1$, while using the prior in (16) for nonparametric additive components.

As an additional note, we comment on the case where one is interested not only in estimation but also in model selection for GAMs by examining the posterior probability that some predictor variables have the linear effect. This is easily accomplished by investigating $\Pi(|\xi_j| = 0 \mid Y)$ in the collected MCMC draws. However, we highlight that the prior in (16) is tailored for the estimation problem of GAMs and should be carefully used for such a model selection purpose. More explicitly, the prior in (16) induces $\Pi(|\xi_j| = 0) = \varpi / [1 - (1 - \varpi)^{M_j+1}] \approx \varpi$ for small ϖ , indicating that small ϖ yields a very informative prior for the linear effect caused by $|\xi_j| = 0$. One might choose ϖ based on a prior belief for the linearity $|\xi_j| = 0$, but this may cause rapid decay for estimation. Another option is considering a mixture-type prior on $|\xi_j|$ ([Jeong et al., 2022](#)). Given that this study focuses on estimation of GAMs, we do not discuss such extensions in detail and direct the reader to [Jeong et al. \(2022\)](#) for further discussion on model selection in additive models.

5 Numerical study

The main objective of this study is to understand how the mixtures of g-priors behave in BMS-based approaches for estimation of GAMs. Section 3.2 provides a basic understanding of how the mixtures of g-priors penalize models. However, it remains unclear which mixture prior is the most appropriate for GAMs. This section provides a simulation study to compare the mixtures

of g-priors for GAM estimation. We also want to examine whether the BMS-based methods outperform other Bayesian approaches for function estimation, for example, Bayesian P-splines.

5.1 Comparison among the mixtures of g-priors

We first conduct a simulation study that reveals the differences among the performances of the mixtures of g-priors for estimation of GAMs. Regarding the synthetic functions, we consider the following three uncentered functions $f_j^* : [-1, 1] \rightarrow \mathbb{R}$, $j = 1, 2, 3$:

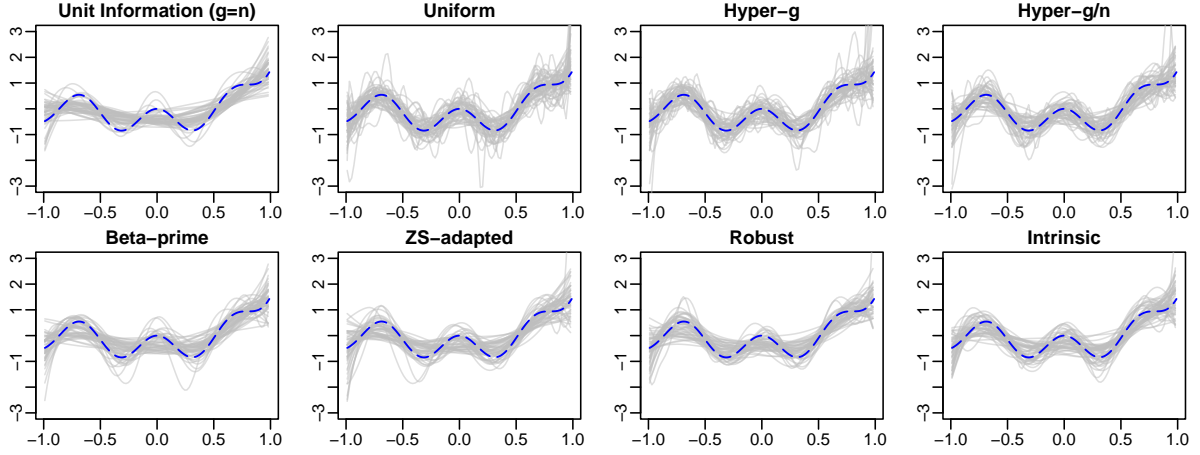
$$\begin{aligned} f_1^*(x) &= 0.5(2x^5 + 3x^2 + \cos(3\pi x) - 1), \\ f_2^*(x) &= \frac{21(3x + 1.5)^3}{8000} + \frac{21(3x - 2.5)^2 e^{3x+1.5}}{400} \sin\left(\frac{(3x + 1.5)^2 \pi}{3.2}\right) \mathbb{1}(-0.5 < x < 0.85), \\ f_3^*(x) &= x. \end{aligned} \quad (17)$$

Specifically, f_1^* is a nonlinear function that is not a polynomial, f_2^* is a nonlinear function with locally varying smoothness, and f_3^* is a linear function. The two nonlinear functions f_1^* and f_2^* are modified from [Gressani and Lambert \(2021\)](#) and [Francom and Sansó \(2020\)](#), respectively. The functions are visualized in Figure 4 with suitable centering.

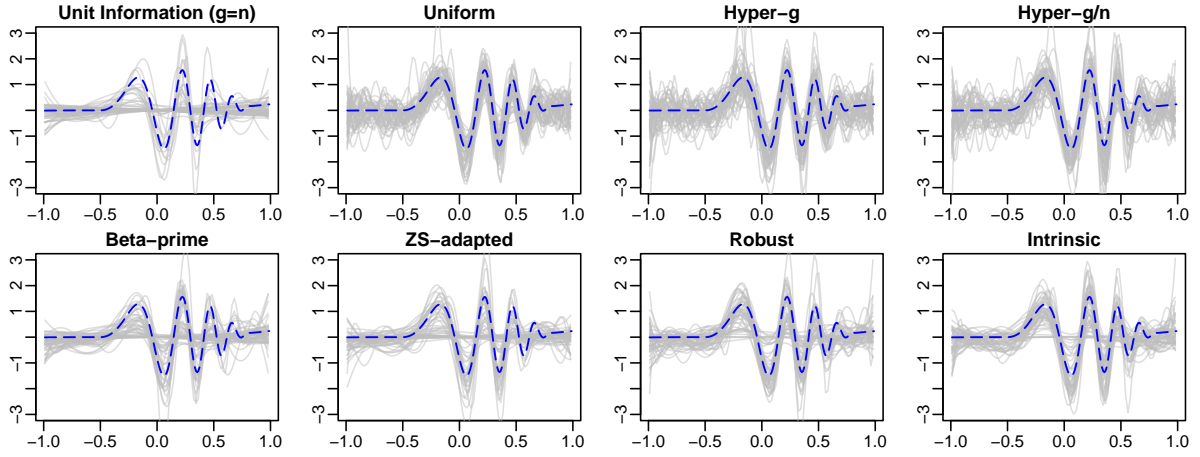
For each $j = 1, 2, 3$, we generate the predictor $\eta_i = f_j^*(x_i) = \alpha + f_j(x_i)$ with x_i drawn independently from $\text{Unif}(-1, 1)$, where f_j is the centered version of f_j^* and α is the induced intercept. The simulation dataset is then generated by the exponential family model with η_i , $i = 1, \dots, n$. In other words, the regression models considered here are not additive but instead comprise a single univariate function. It is certainly possible to carry out simulation using an additive structure but we observe that a single univariate function sharpens the differences among the mixtures of g-priors. In this section, we only provide a simulation result for a nonlinear logistic regression model given by $Y_i \sim \text{Bernoulli}(e^{\eta_i}/(1 + e^{\eta_i}))$. The supplementary material includes simulation studies for Poisson regression $Y_i \sim \text{Poi}(e^{\eta_i})$.

Among the three strategies for choosing Ξ described in Section 4, we focus on the VS-knot splines approach because we observe that it generally outperforms the other methods in terms of both empirical performance and computational efficiency (the three strategies are compared in Section 5.2). For each of the logistic regression models with $n = 500, 1000, 2000$, we generate 500 replications of datasets and estimate f_j using the VS-knot splines comprising 30 knot candidates with the unit information prior and the mixture priors summarized in Table 1. We calculate the root mean squared error (RMSE) and the coverage probabilities of the 95% pointwise credible bands at a few given points.

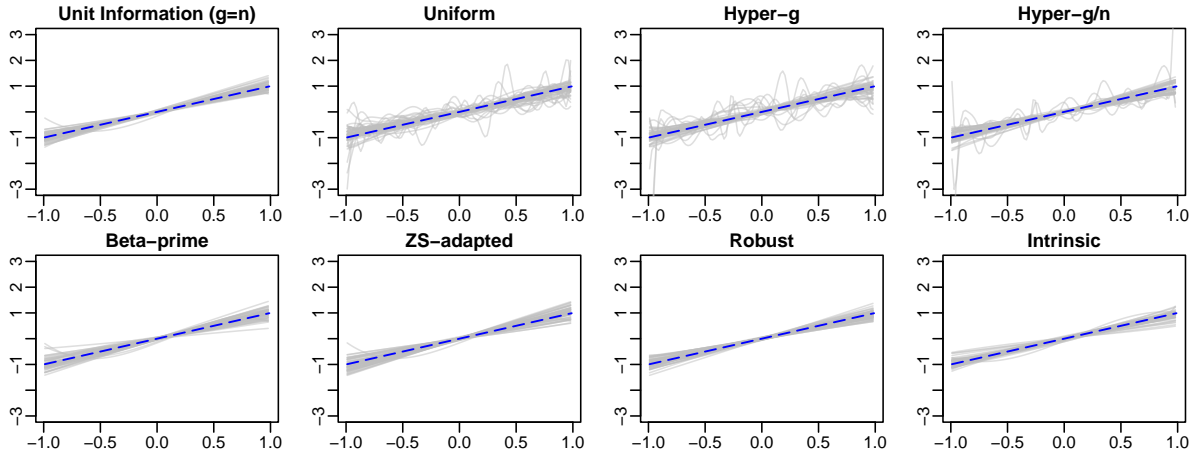
Figures 4 and 5 summarize the simulation results. As discussed in Section 3.2, the unit information prior behaves very differently from the mixture priors; it generally underperforms for nonlinear function estimation and exhibits clear oversmoothing. This indicates that the convention of employing the unit information prior for function estimation may be inappropriate. The major challenge is determining which mixture prior is the most suited for function estimation. Based on our simulation analysis, we conclude that the intrinsic and robust priors are the most suitable choices. Although the difference between the mixtures of g-priors is blurred for a large sample size, it is quite that intrinsic and robust priors almost always outperform the other priors across finite samples; the beta-prime and ZS-adapted priors tend to exhibit undersmoothing,



(a) Pointwise posterior mean estimates of f_1 in 50 replications



(b) Pointwise posterior mean estimates of f_2 in 50 replications



(c) Pointwise posterior mean estimates of f_3 in 50 replications

Figure 4: Estimates of (a) f_1 , (b) f_2 , and (c) f_3 in the nonparametric logistic regression models with $n = 500$. Pointwise posterior means of randomly chosen 50 replications (gray solid) and true function (blue dashed).

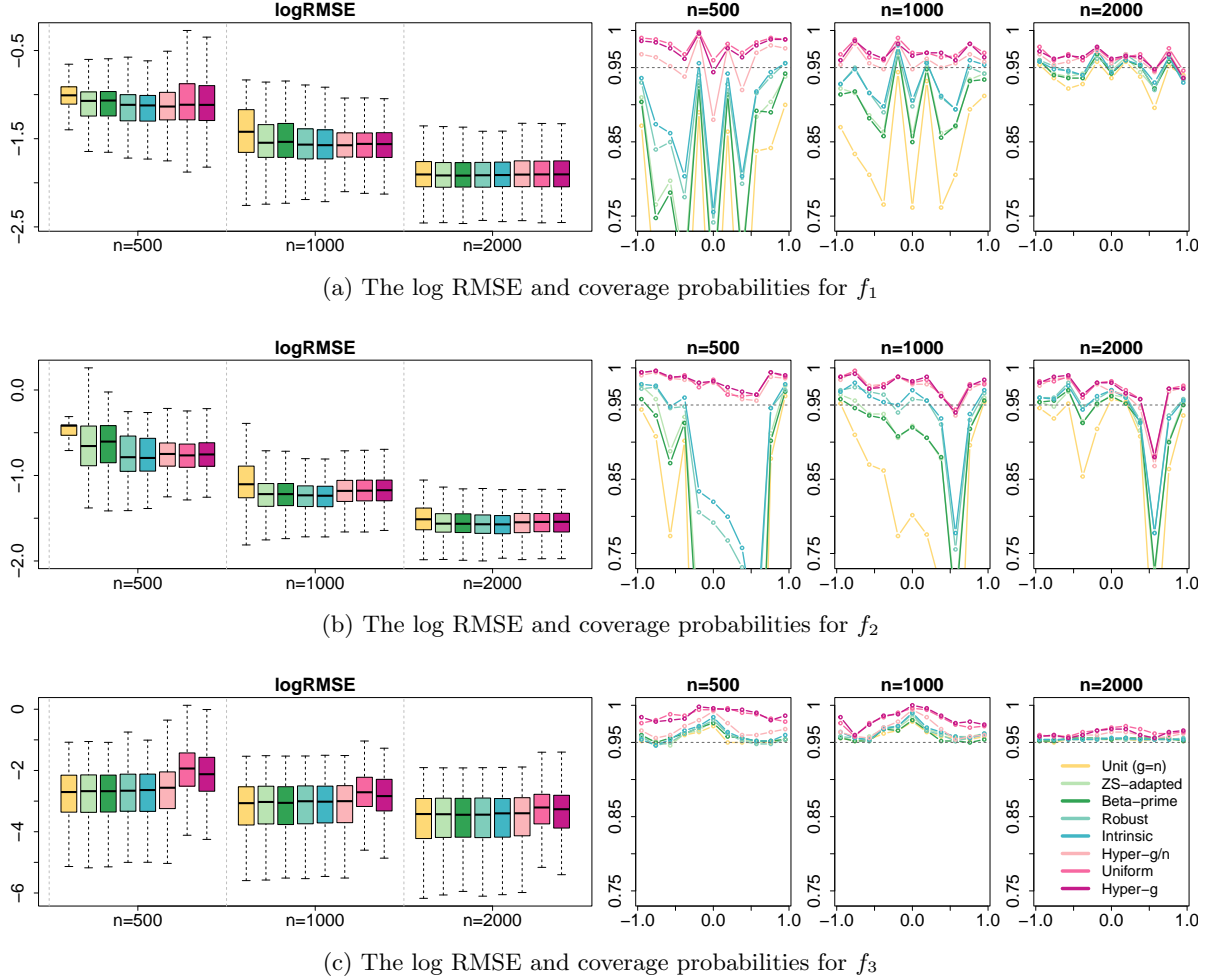
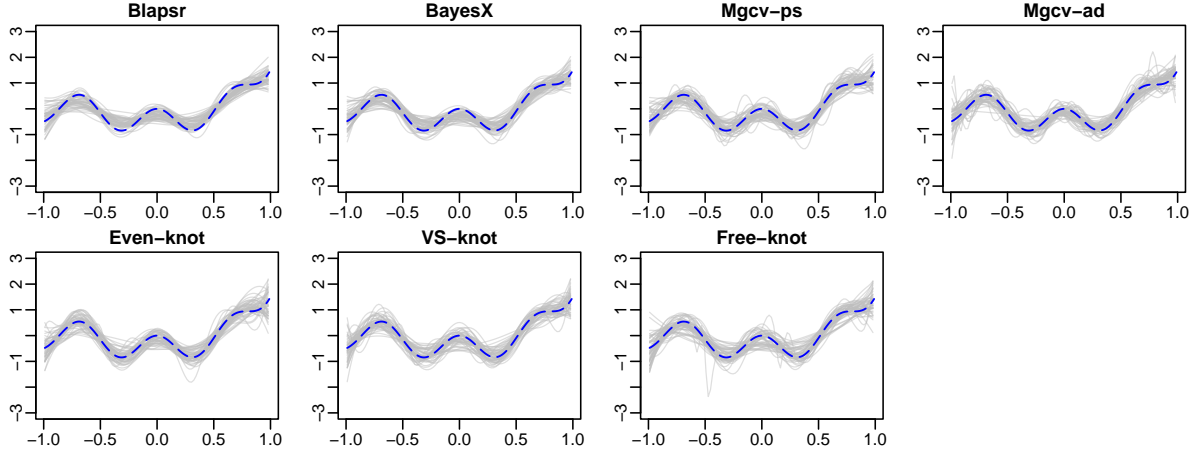


Figure 5: The log RMSE and coverage probabilities for (a) f_1 , (b) f_2 , and (c) f_3 in the nonparametric logistic regression models with $n = 500, 1000, 2000$.

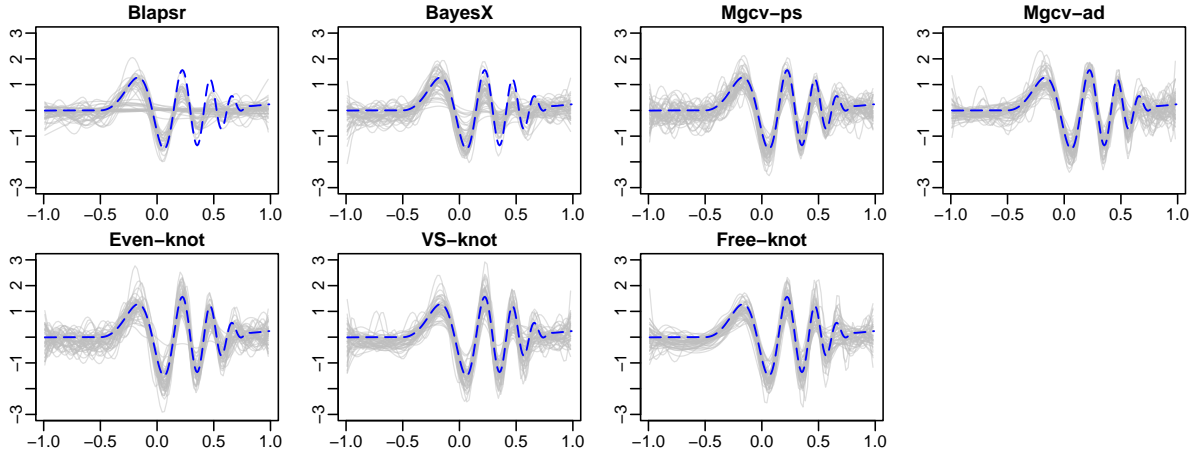
whereas the uniform, hyper- g , and hyper- g/n priors tend to exhibit oversmoothing. The simulation results for Poisson regression in the supplementary material also provide a similar conclusion. The remaining question is how to determine the default prior between the intrinsic and robust priors. As discussed in the last paragraph of Section 3.1, sampling from the posterior distribution of g is facilitated with the robust prior. Therefore, we choose the robust prior as our default prior for a hierarchy of g .

5.2 Comparison with other methods

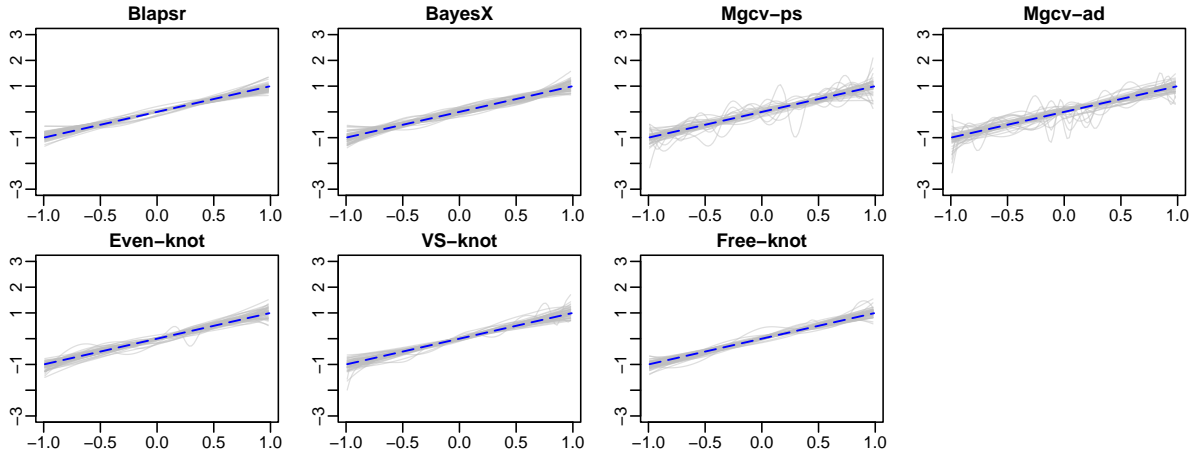
Now, we compare the BMS-based methods for GAMs with other Bayesian methods for function estimation. We consider the three strategies described in Section 4: the even-knot splines, VS-knot splines, and free-knot splines, along with a few Bayesian competitors available in R packages: R2BayesX (Umlauf et al., 2012), Blapsr (Gressani and Lambert, 2021), and mgcv (Wood, 2017). The BMS-based approaches are equipped with the robust prior based on the simulation study in Section 5.1. Given that all competitors are based on Bayesian P-splines (Lang and Brezger, 2004),



(a) Pointwise posterior mean estimates of f_1 in 50 replications



(b) Pointwise posterior mean estimates of f_2 in 50 replications



(c) Pointwise posterior mean estimates of f_3 in 50 replications

Figure 6: Estimates of (a) f_1 , (b) f_2 , and (c) f_3 in the nonparametric logistic regression model with $n = 1000$. Pointwise posterior means of randomly chosen 50 replications (gray solid) and true functions (blue dashed).

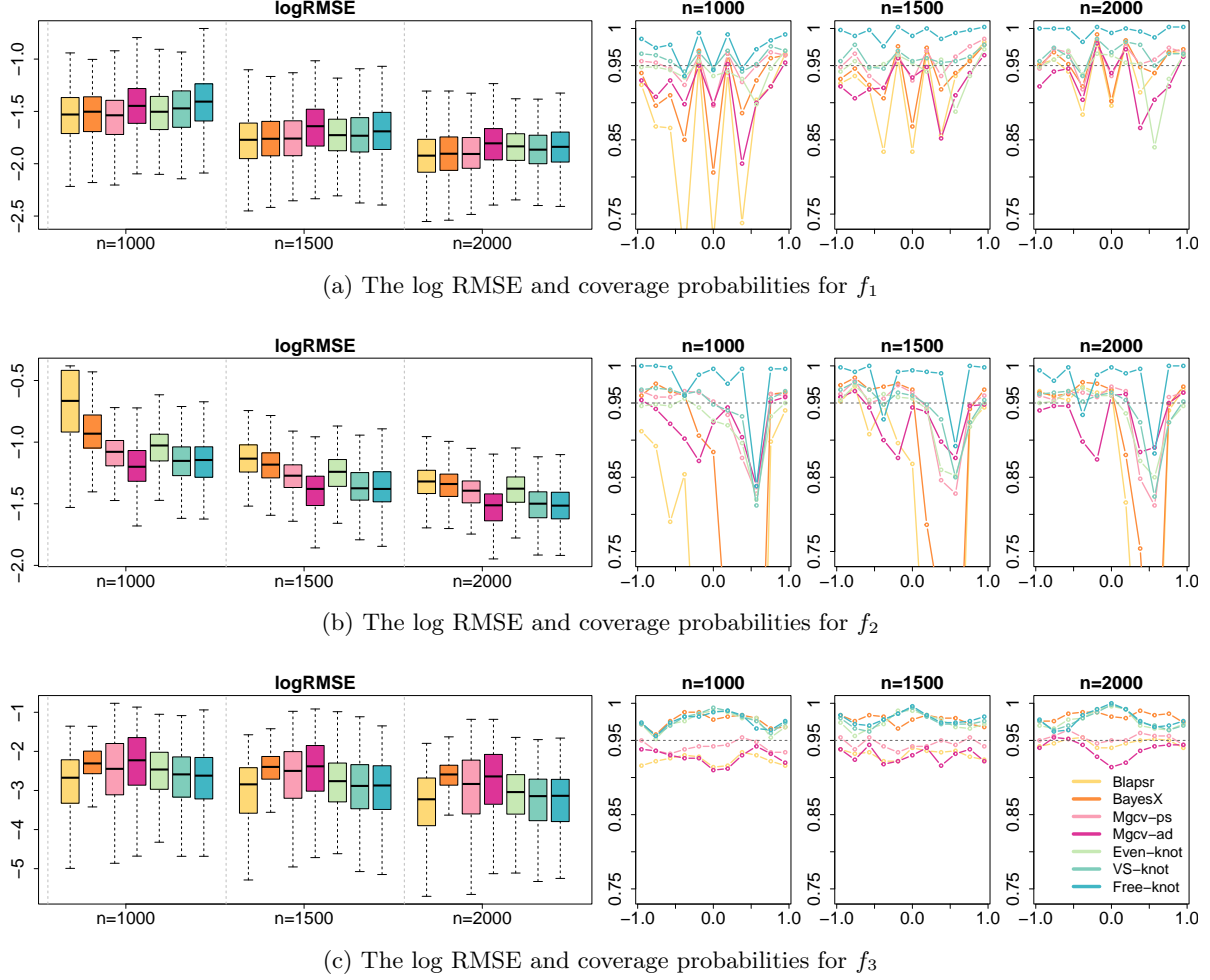


Figure 7: The log RMSE and coverage probabilities for (a) f_1 , (b) f_2 , and (c) f_3 in the nonparametric logistic regression models with $n = 1000, 1500, 2000$.

they are intrinsically different from the BMS-based approaches at a philosophical level. The differences in the competitors arise from how they handle the smoothness parameters. Whereas `R2BayesX` provides standard MCMC estimates, `Blapsr` has an option to utilize the Laplace approximation for a small number of additive components to facilitate computation. In general, `mgcv` is fastest and most computationally efficient; however, it is not fully Bayesian because it resorts to the generalized cross-validation in choosing the smoothness parameters. The simulation specification is carefully chosen for a fair comparison among the methods. For the BMS-based approaches (i.e., the even-knot, VS-knot, and free-knot splines), the maximum number of knots M_j is fixed to 30 for every $j = 1, 2, 3$. We also use $M_j = 30$ for the competitors that are based on Bayesian P-splines (i.e., `R2BayesX`, `Blapsr`, and `mgcv`), so that both the BMS-based approaches and Bayesian P-spline approaches have comparable least penalized models. The `mgcv` package provides an option to pursue locally adaptive estimation for smooth functions.

Using the functions in (17), the simulation datasets are generated by the additive predictor $\eta_i = \sum_{j=1}^3 f_j^*(x_{ij}) = \alpha + \sum_{j=1}^3 f_j(x_{ij})$ with x_{ij} drawn independently from $\text{Unif}(-1, 1)$, where f_j

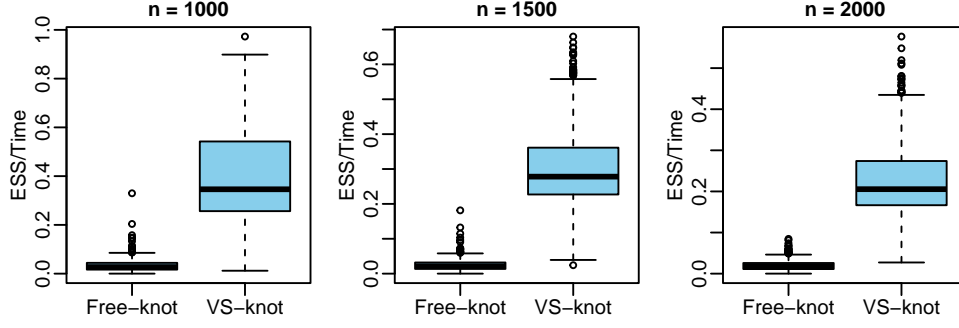


Figure 8: The efficiency ratio, the number of effective sample per one second of CPU runtime, in the nonparametric logistic regression models with $n = 1000, 1500, 2000$ for VS-knot and free-knot.

is the centered version of f_j^* in (17) and α is the induced intercept. For the nonlinear logistic regression model $Y_i \sim \text{Bernoulli}(e^{\eta_i}/(1 + e^{\eta_i}))$, 500 replicated datasets are generated with $n = 1000, 1500, 2000$. We also consider Poisson regression $Y_i \sim \text{Poi}(e^{\eta_i})$ whose simulation results are provided in the supplementary material. Similar to Section 5.1, we calculate the RMSE and 95% pointwise credible bands at a few given points for each method.

Figures 6 and 7 summarize the simulation results for the nonlinear logistic regression models. Observing the figures, one can easily conclude that **R2BayesX** and **Blapsr** often oversmooth the target functions with excessive penalization. Conversely, **mgcv** provides extremely wiggly estimates of the linear function, meaning that the method often leads to undersmoothing for simple functions. As seen in Figures 6 and 7, **R2BayesX** and **Blapsr** do not work properly for locally varying smoothness. This is to be expected given that Bayesian P-splines are not designed for locally adaptive estimation without major modifications (Crainiceanu et al., 2007; Jullion and Lambert, 2007; Scheipl and Kneib, 2009). We observe that **mgcv** with local adaptation performs very well for estimation of locally varying smoothness. However, as can be seen from the performance summaries for f_1 and f_3 , the use of **mgcv** for adaptive estimation may lead to higher RMSEs and incorrect coverage probabilities. The major drawback of **mgcv** is that the use of adaptive estimation must be correctly specified in advance for optimal performance. Such a characteristic of the target function is generally unknown to us. The results for Poisson regression in the supplementary material also lead to a similar conclusion.

Among the BMS-based approaches, the even-knot splines cannot adapt to locally varying smoothness of f_2 because of their simple construction with equidistant knots. In contrast, the log RMSEs show that both the VS-knot and free-knot splines correctly detect the local features of f_2 ; the RMSEs of the two methods for adaptive estimation are very similar unless the target function is extremely complicated. However, one may see that the coverage probabilities induced by the free-knot splines are too close to 1. We observe that this is because a design matrix generated by the free-knot splines often becomes numerically singular although it is nonsingular, leading to severe numerical errors in calculating the covariance matrix. The VS-knot splines are much more stable and free of this issue. Moreover, we find that the VS-knot splines outperform the free-knot splines in terms of sampling efficiency (measured as the ratio of effective sample size to runtime), as shown in Figure 8. Compared to **mgcv**, the VS-knot approach does not require the

correct determination for the use of adaptive estimation, while outperforming the competitors in most cases. Therefore, we recommend the VS-knot splines as the default option. Nonetheless, it is worth mentioning that the even-knot splines approach is faster than the other BMS-based methods and also eliminates the need for MCMC when p is reasonably small.

6 Discussion

This study considers BMS-based estimation methods for GAMs using the Laplace approximation with mixtures of g-priors. To determine a default prior for knots and a default mixture prior, we provide an interpretation of mixtures of g-priors as penalty functions and various numerical results. As a byproduct of doing so, the existing ideas on priors for knots and mixtures of g-priors are collectively collated in the study.

The major bottleneck of our BMS-based approaches is the dependency on the maximum likelihood estimator, which leads to costly computation. Given that the VS-knot splines approach is shown to be sufficiently effective in this study, a possible remedy is employing shrinkage priors for exponential family models with a reasonable MCMC sampling algorithm (e.g., [Schmidt and Makalic, 2020](#)). Another possibility is using a computationally less expensive approximation to the likelihood (e.g., [Rossell et al., 2021](#)). We consider using the latter for future research.

Acknowledgment

The research was supported by the Yonsei University Research Fund of 2021-22-0032 and the National Research Foundation of Korea (NRF) grant funded by the Korea government (MSIT) (NRF-2022R1C1C1006735).

Supplementary material

A Truncated compound confluent hypergeometric distributions

The truncated compound confluent hypergeometric (tCCH) distribution is formally defined by [Li and Clyde \(2018\)](#), as a slight modification of the generalized beta distribution defined by [Gordy \(1998b\)](#). Specifically, we write $U \sim \text{tCCH}(a, b, z, s, \nu, \kappa)$ if U has a density of the form

$$f(u) = \frac{\nu^a u^{a-1} (1 - \nu u)^{b-1} [\kappa + (1 - \kappa)\nu u]^{-z} e^{s/\nu} e^{-su}}{\Phi_1(b, z, a + b, s/\nu, 1 - \kappa) B(a, b)} \mathbb{1}(0 < u < 1/\nu). \quad (18)$$

A direct calculation gives the k th moment as

$$E(U^k) = \nu^{-k} \frac{B(a + k, b) \Phi_1(b, z, a + b + k, s/\nu, 1 - \kappa)}{B(a, b) \Phi_1(b, z, a + b, s/\nu, 1 - \kappa)}. \quad (19)$$

The tCCH distribution is a type of generalized beta distributions with five parameters that allow for a multi-modal or long-tailed density. The parameters a and b behave similarly to the parameters of a beta distribution. The parameters z , s , and κ determine the skewness of the density and the parameter ν determines the support.

The tCCH distribution reduces to many distributions depending on the parameter values, such as a Gaussian hypergeometric distribution ([Armero and Bayarri, 1994](#)), confluent hypergeometric distribution ([Gordy, 1998a](#)), beta distribution, and gamma distribution. We refer the reader to the monograph [Gupta and Nadarajah \(2004, p.132, p.279\)](#) for more details. Accordingly, the marginal likelihood in (11) is simplified depending on the parameters of the tCCH prior.

B Exact sampling from tCCH distributions

Given (18), the density function of $\text{tCCH}(a, 1, z, s, \nu, 1)$ has the form $f(u) \propto u^{a-1} e^{-su} \mathbb{1}(0 < u < 1/\nu)$, which is the gamma density truncated to $0 < u < 1/\nu$. Therefore, exact sampling from tCCH distributions is straightforward using the inverse transform method in this specific case. Combining the first line of (12) and Table 1, it is trivial that the posterior distribution $\Pi((g + 1)^{-1} \mid Y, \xi)$ is reduced to a truncated gamma distribution if the uniform, hyper-g, ZS-adapted, or robust priors is used.

C Proofs of the propositions

Proof of Proposition 1. Consider boundary knots $\{t^L, t^U\}$ and interior knots $\{t_1, \dots, t_M\}$ satisfying $t^L < t_1 < \dots < t_M < t^U$. To concatenate the expressions, we write $t_0 = t^L$ and $t_{M+1} = t^U$. The common expression of the natural cubic splines derived from the truncated cubic spline basis functions is given by

$$N_1^*(u) = u, \\ N_{k+2}^*(u) = \frac{(u - t_k)_+^3 - (u - t_{M+1})_+^3}{t_{M+1} - t_k} - \frac{(u - t_M)_+^3 - (u - t_{M+1})_+^3}{t_{M+1} - t_M}, \quad k = 0, \dots, M - 1,$$

(see, for example, equations (5.4) and (5.5) of [Hastie et al. \(2009\)](#)). Letting $N_0^*(u) = 1$, it is well known that $\mathcal{N}^* = \{N_k^*, k = 0, 1, \dots, M+1\}$ is a basis for the cubic spline space with the natural boundary conditions. Therefore, it suffices to show that there exists an injection $Q : \mathcal{N} \mapsto \mathcal{N}^*$. As $N_0 = N_0^*$, $N_1 = N_1^*$, $-N_{M+1} = N_2^*$ and $N_{k-1} - N_{M+1} = N_k^*$, $k = 3, \dots, M+1$, we obtain

$$Q = \begin{pmatrix} 1 & 0 & 0 & 0 & \dots & 0 & 0 \\ 0 & 1 & 0 & 0 & \dots & 0 & 0 \\ 0 & 0 & 0 & 0 & \dots & 0 & -1 \\ 0 & 0 & 1 & 0 & \dots & 0 & -1 \\ 0 & 0 & 0 & 1 & \dots & 0 & -1 \\ \vdots & \vdots & \vdots & \vdots & \ddots & \vdots & \vdots \\ 0 & 0 & 0 & 0 & \dots & 1 & -1 \end{pmatrix},$$

which is clearly nonsingular. \square

Proof of Proposition 2. Observe that each of the basis terms $N(\cdot; t^L, t^U, t_k)$, $k = 1, \dots, M$, in \mathcal{N} consists only of t^L , t^U , and t_k . Hence, a new knot-point t_* introduces a new basis that is defined as $N(\cdot; t^L, t^U, t_*)$ without altering other basis terms. Similarly, the elimination of an existing knot-point t_k removes the corresponding $N(\cdot; t^L, t^U, t_k)$ without altering other terms. \square

Proof of Proposition 3. If $\hat{\eta}_{\xi_1} = \hat{\eta}_{\xi_2}$, one can easily observe that

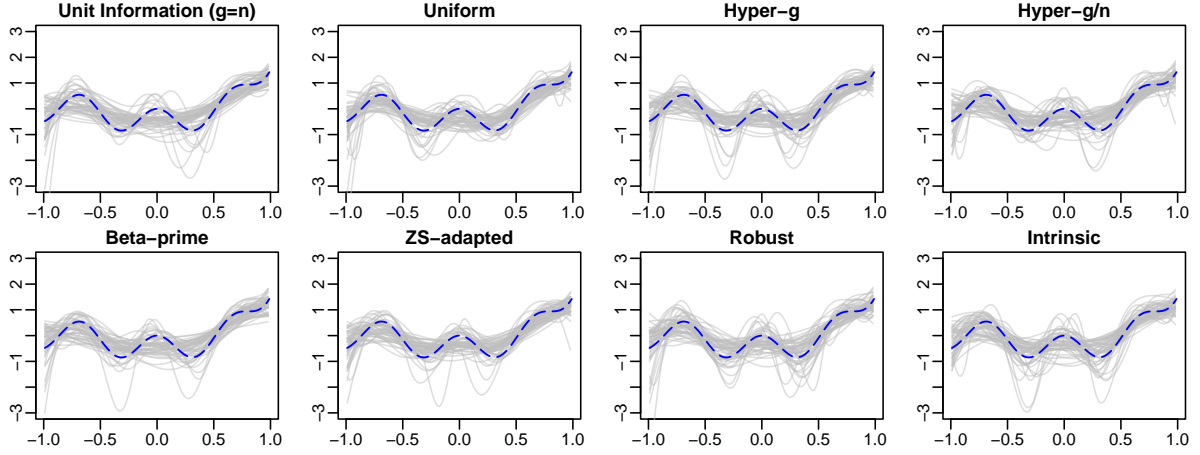
$$BF[\xi_1; \xi_2] = \nu^{-k/2} \frac{B((a + J_{\xi_1})/2, b/2) \Phi_1(b/2, r, (a + b + J_{\xi_1})/2, (s + Q_{\xi_1})/(2\nu), 1 - \kappa)}{B((a + J_{\xi_2})/2, b/2) \Phi_1(b/2, r, (a + b + J_{\xi_2})/2, (s + Q_{\xi_2})/(2\nu), 1 - \kappa)},$$

using the expression in (11). Given that the posterior of $(g+1)^{-1}$ is the tCCH distribution in (12), the assertion is easily verified using (19) if the tCCH prior is used for $(g+1)^{-1}$. For the unit information prior, the result can be proved in a similar manner. \square

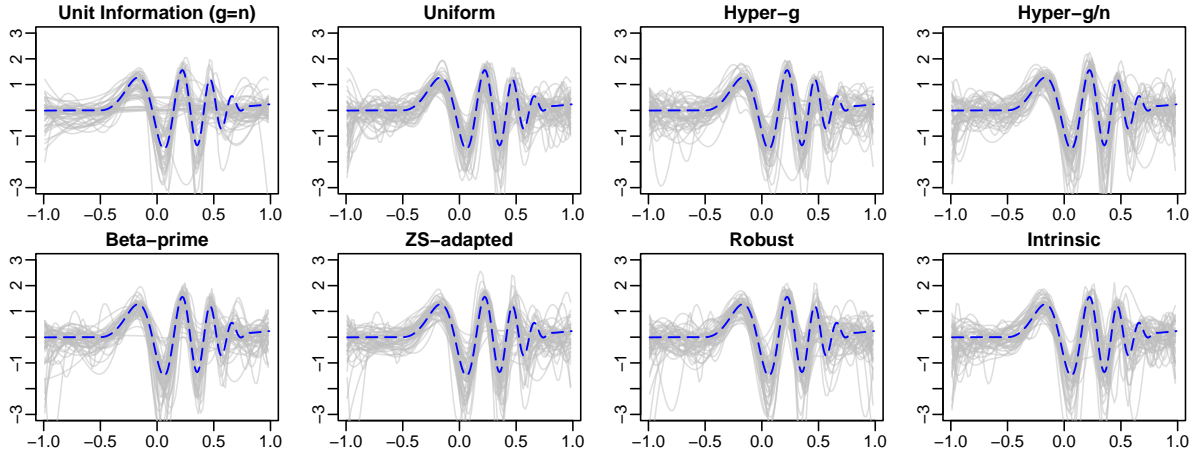
D Additional simulation study for Poisson regression

We present additional simulation results for the Poisson regression models. To compare the mixtures of g-priors, similar to Section 5.1, the observations are generated from $Y_i \sim \text{Poi}(e^{\eta_i})$ with the predictor $\eta_i = f_j^*(x_i) = \alpha + f_j(x_i)$ using f_j , the centered version of f_j^* in (17), and the induced intercept α . For each of $j = 1, 2, 3$, we generate 500 replicated datasets for $n = 100, 200, 300$. As a result, the Poisson regression models used here are not additive but instead comprise univariate functions for their mean responses. The simulation results are provided in Figures 9 and 10. The differences among the mixture priors are not as obvious as they are in Section 5.1; however, the overall trends are comparable, leading to the similar conclusion.

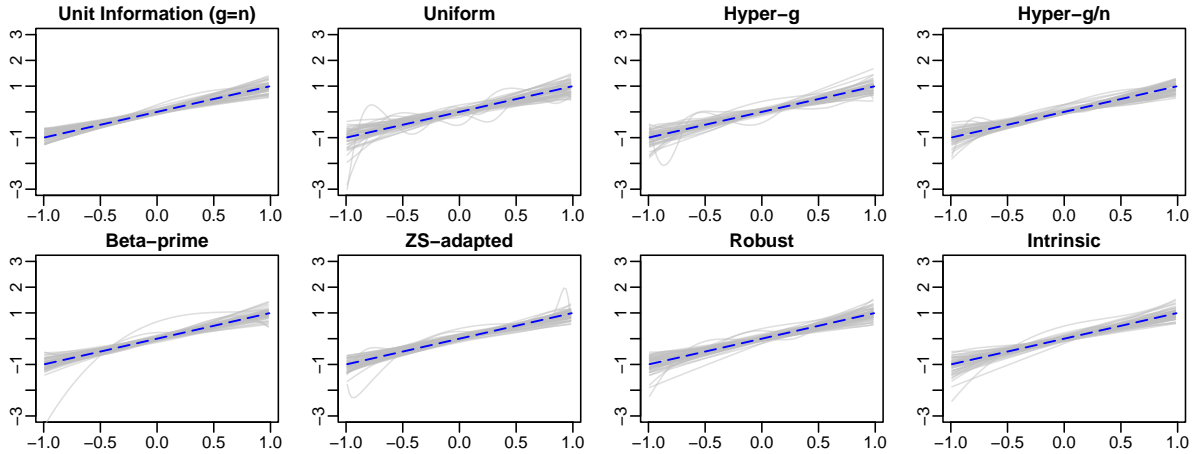
To compare the BMS-based methods with other Bayesian approaches, the observations are now generated by the additive predictor $\eta_i = \sum_{j=1}^3 f_j^*(x_{ij}) = \alpha + \sum_{j=1}^3 f_j(x_{ij})$. Similar to the aforementioned case, 500 replicated datasets are generated for $n = 100, 200, 300$. The simulation results are summarized in Figures 11 and 12. The results are similar to those in Section 5.2 and we reach a comparable conclusion.



(a) Pointwise posterior mean estimates of f_1 in 50 replications



(b) Pointwise posterior mean estimates of f_2 in 50 replications



(c) Pointwise posterior mean estimates of f_3 in 50 replications

Figure 9: Estimates of (a) f_1 , (b) f_2 , and (c) f_3 in the nonparametric poisson regression models with $n = 100$. Pointwise posterior means of randomly chosen 50 replications (gray solid) and true function (blue dashed).

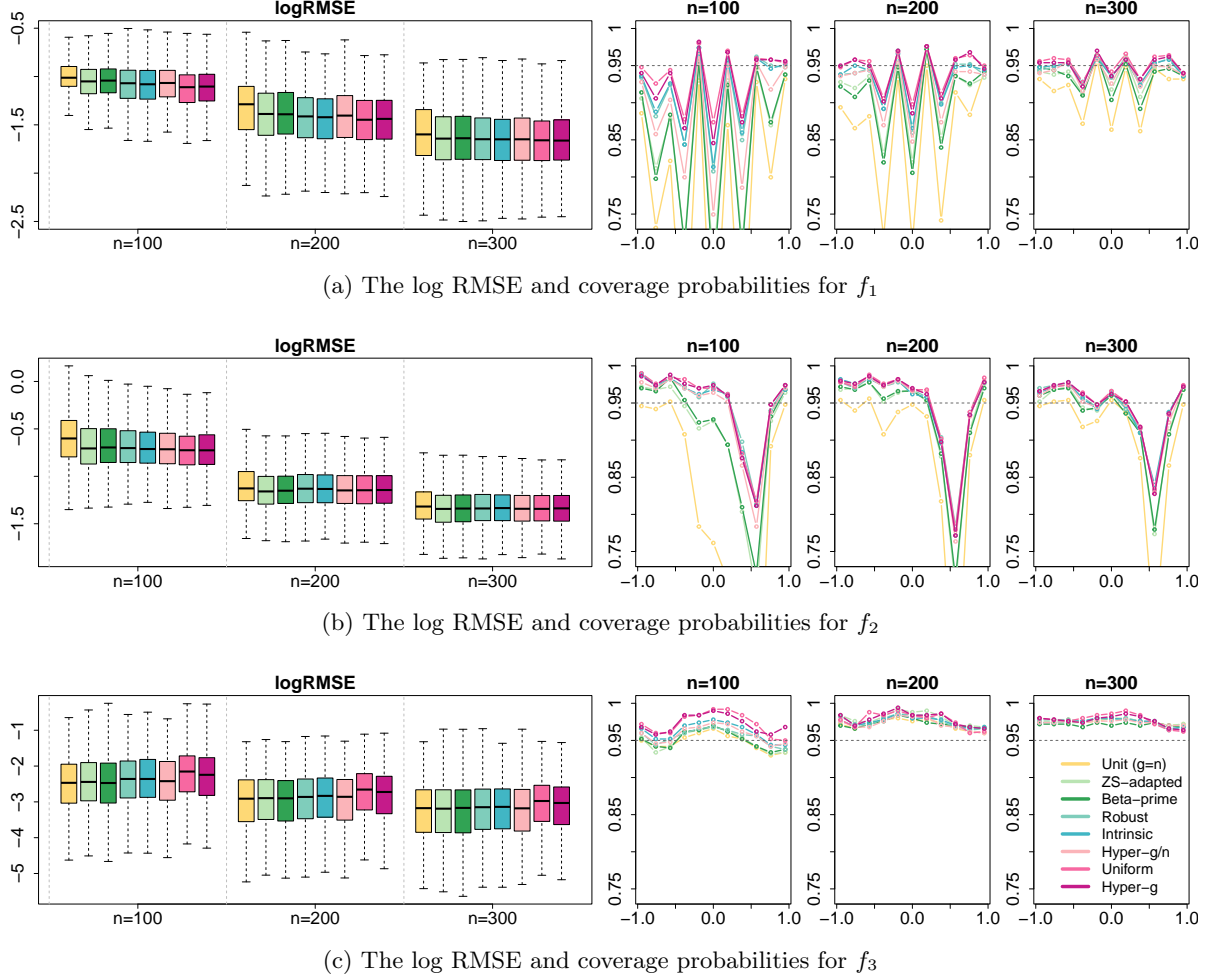


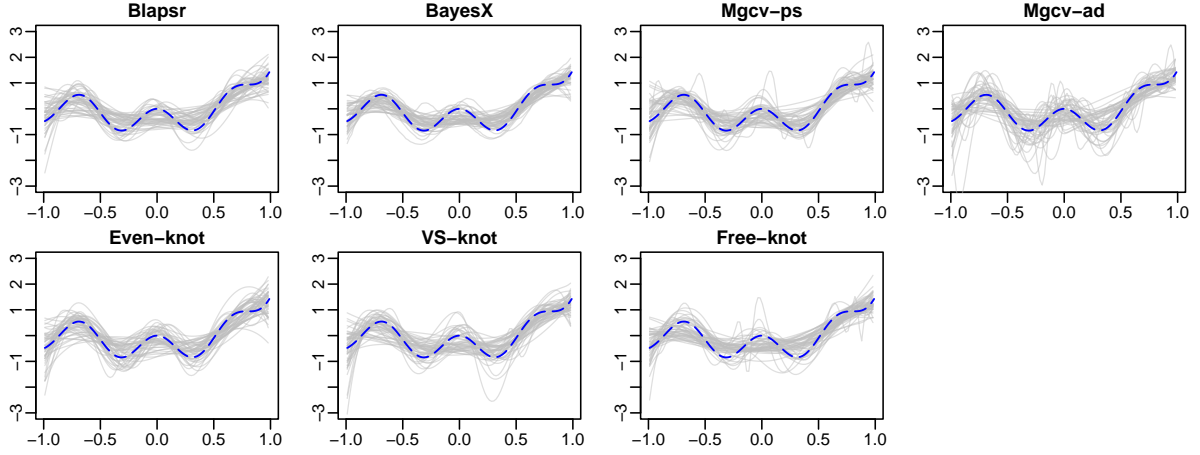
Figure 10: The log RMSE and coverage probabilities for (a) f_1 , (b) f_2 , and (c) f_3 in the non-parametric poisson regression models with $n = 100, 200, 300$.

E Gaussian additive regression with unknown precision

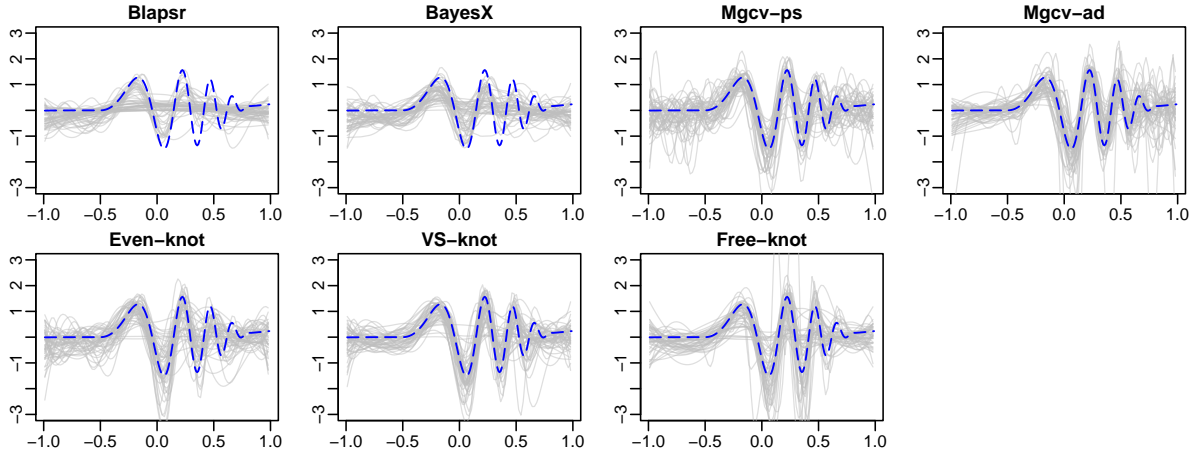
Thus far, we have focused on GAMs with known dispersion parameter ϕ for the exponential family models. Now we consider a more classical setup with a Gaussian assumption on the distribution of Y_i , while treating ϕ as an unknown parameter. For Gaussian additive regression, a response variable Y_i is expressed as

$$Y_i = \alpha + \sum_{j=1}^p f_j(x_{ij}) + \epsilon_i, \quad \epsilon_i \sim N(0, \phi^{-1}), \quad i = 1, \dots, n, \quad (20)$$

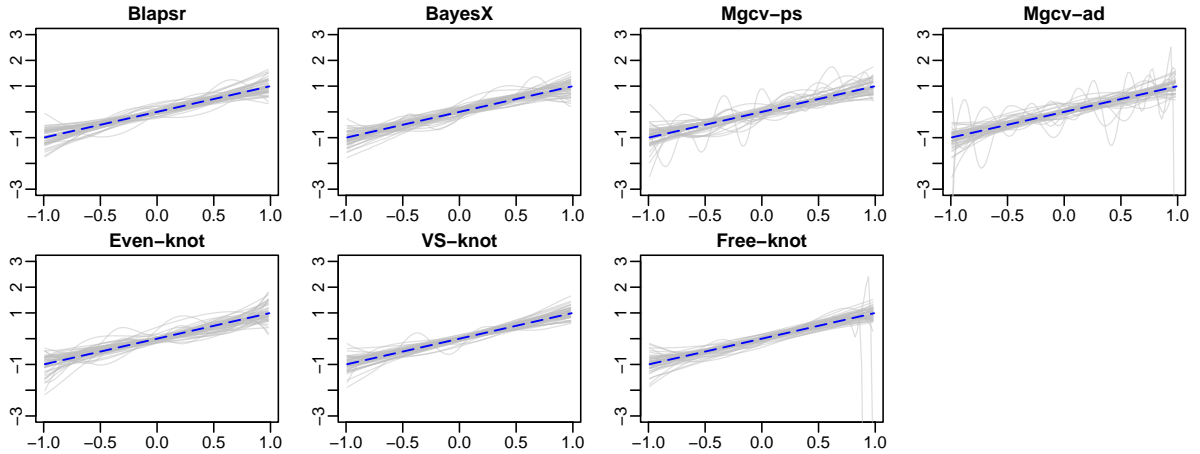
where the precision parameter ϕ is typically unknown. Although model (20) also belongs to the GAM framework, things are different because of the unknown precision ϕ . Let $\eta = (\eta_1, \dots, \eta_n)^T$ be the vector of mean response, that is, $\eta_i = E(Y_i)$. We parameterize η as $\eta = \alpha \mathbf{1}_n + B_\xi \beta_\xi$ with α , B_ξ , and β_ξ as defined in Section 2. Following the convention, an improper prior is put on



(a) Pointwise posterior mean estimates of f_1 in 50 replications



(b) Pointwise posterior mean estimates of f_2 in 50 replications



(c) Pointwise posterior mean estimates of f_3 in 50 replications

Figure 11: Estimates of (a) f_1 , (b) f_2 , and (c) f_3 in the nonparametric poisson regression model with $n = 100$. Pointwise posterior means of randomly chosen 50 replications (gray solid) and true functions (blue dashed).

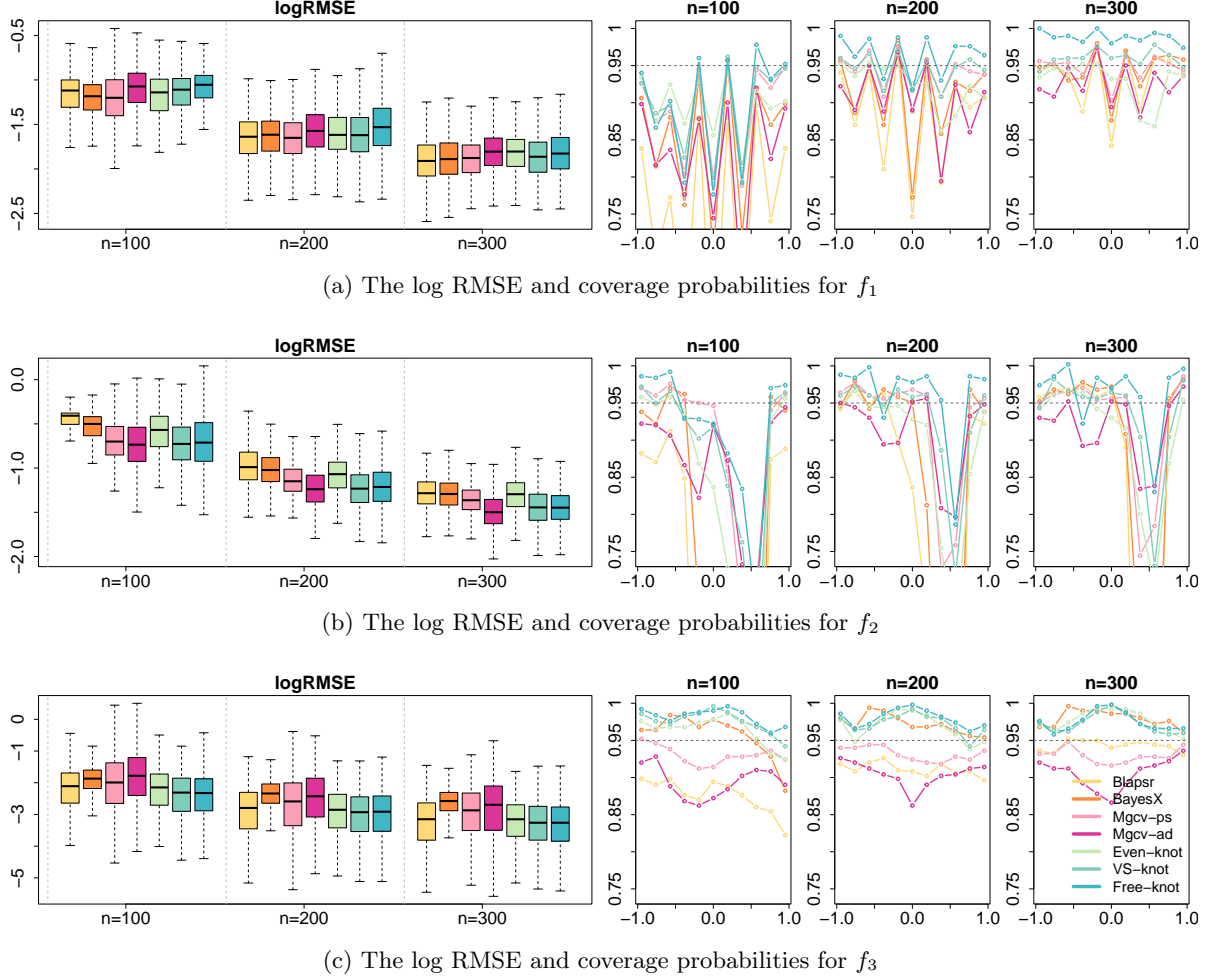


Figure 12: The log RMSE and coverage probabilities for (a) f_1 , (b) f_2 , and (c) f_3 in the non-parametric poisson regression models with $n = 100, 200, 300$.

(α, ϕ) , that is,

$$\pi(\alpha, \phi) \propto 1/\phi.$$

Given that the information matrix of a Gaussian distribution is an identity matrix, one can easily check that the prior in (8) is reduced to the usual g-prior distribution (Zellner, 1986),

$$\beta_\xi \mid \phi, g, \xi \sim N(0, g\phi^{-1}(B_\xi^T B_\xi)^{-1}).$$

(For the Gaussian case, we obtain $\tilde{B}_\xi = B_\xi$ because the columns of B_ξ are centered.)

Combining the marginal likelihood with one of the priors on ξ discussed in Section 4, we obtain the marginal posterior of ξ , $\Pi(\xi \mid Y)$. The calculation of the marginal likelihood is complicated because ϕ needs to be integrated along with g . First, it is well known that

$$p(Y \mid g, \xi) = p(Y \mid \emptyset) \frac{(1+g)^{(n-J_\xi-1)/2}}{[1+g(1-R_\xi^2)]^{(n-1)/2}}, \quad (21)$$

where $p(Y | \varnothing) = n^{-1/2}(2\pi)^{-(n-1)/2}\Gamma((n-1)/2)(\|Y - \bar{Y}1_n\|^2/2)^{-(n-1)/2}$ is the marginal likelihood in the intercept-only model, $R_\xi^2 = \|B_\xi(B_\xi^T B_\xi)^{-1}B_\xi^T Y\|^2/\|Y - \bar{Y}1_n\|^2$ is the coefficient of determination with ξ , and $\bar{Y} = n^{-1}\sum_{i=1}^n Y_i$ is the average of the observations. For the unit information prior $\Pi(g) = \delta_n(g)$, the marginal likelihood $p(Y | \xi)$ is readily available from the expression in (21). Assigning the tCCH prior in (10) to $(g+1)^{-1}$, Li and Clyde (2018) shows that if $r = 0$ (or $\kappa = 1$ equivalently),

$$p(Y | \xi) = \frac{p(Y | \varnothing)}{\nu^{J_\xi/2}[1 - (1 - \nu^{-1})R_\xi^2]^{(n-1)/2}} \frac{B((a + J_\xi)/2, b/2)}{B(a/2, b/2)} \\ \times \Phi_1\left(\frac{b}{2}, \frac{n-1}{2}, \frac{a+b+J_\xi}{2}, \frac{s}{2\nu}, \frac{R_\xi^2}{\nu - (\nu-1)R_\xi^2}\right) / {}_1F_1\left(\frac{b}{2}, \frac{a+b}{2}, \frac{s}{2\nu}\right),$$

and if $s = 0$,

$$p(Y | \xi) = \frac{p(Y | \varnothing)\kappa^{(a+J_\xi-2r)/2}}{\nu^{J_\xi/2}(1 - R_\xi^2)^{(n-1)/2}} \frac{B((a + J_\xi)/2, b/2)}{B(a/2, b/2)} \\ \times F_1\left(\frac{a + J_\xi}{2}; \frac{a+b+J_\xi+1-n-2r}{2}, \frac{n-1}{2}; \right. \\ \left. \frac{a+b+J_\xi}{2}; 1-\kappa, 1-\kappa - \frac{R_\xi^2\kappa}{(1-R_\xi^2)v}\right) / {}_2F_1\left(r, \frac{b}{2}; \frac{a+b}{2}; 1-\kappa\right),$$

where ${}_1F_1(\alpha, \gamma, x) = \Phi_1(\alpha, 0, \gamma, x, 0)$ is the confluent hypergeometric function, ${}_2F_1(\beta, \alpha; \gamma; y) = \Phi_1(\alpha, \beta, \gamma, 0, y)$ is the Gaussian hypergeometric function, and F_1 is the the Appell hypergeometric function defined as $F_1(\alpha; \beta, \beta'; \gamma; x, y) = B(\gamma - \alpha, \alpha)^{-1} \int_0^1 u^{\alpha-1}(1-u)^{\gamma-\alpha-1}(1-xu)^{-\beta}(1-yu)^{-\beta'} du$. The prior distributions listed in Table 1 belong to either one of the above two cases. The expressions may further be simplified depending on the hyperparameters of the tCCH prior, but numerical evaluation of the transcendental functions is mostly required. The only exception is the beta-prime prior, which provides a closed-form expression for the marginal likelihood without a hypergeometric-type transcendental function; see Maruyama and George (2011).

For the Gaussian case, the conditional posterior $\Pi((g+1)^{-1} | Y, \xi)$ is no longer a conjugate update of the tCCH prior. Nonetheless, it is simplified with some hyperparameter specification of the tCCH prior and sampling from $\Pi((g+1)^{-1} | Y, \xi)$ is easily carried out by introducing auxiliary variables. In particular, the beta-prime prior provides an exact sampling scheme from a beta distribution; see Jeong et al. (2022). The remaining specification of the joint posterior can easily be derived by direct calculations as

$$\phi | Y, g, \xi \sim \text{Gamma}\left(\frac{n-1}{2}, \frac{\|Y - \bar{Y}1_n\|^2[1 + g(1 - R_\xi^2)]}{2(1+g)}\right), \\ \alpha | Y, \phi, g, \xi \sim N(\bar{Y}, \phi^{-1}/n), \\ \beta_\xi | Y, \phi, g, \xi \sim N\left(\frac{g}{g+1}\hat{\beta}_\xi, \frac{g\phi^{-1}}{g+1}(B_\xi^T B_\xi)^{-1}\right).$$

The marginal posterior of ξ , $\Pi(\xi | Y)$, is easily obtained from the above expressions of the marginal likelihood.

Parameter	Mean	Median	95% lower limit	95% upper limit
α	-1.1567	-1.1556	-1.4039	-0.9066

Table 2: Summary statistics of the posterior distribution for the model in (22).

F Application to Pima diabetes data

In this section, we analyze the Pima datasets using the VS-knot splines approach with the robust prior. The Pima diabetes dataset consists of signs of diabetes and seven potential risk factors of $n = 532$ Pima Indian women in Arizona (Smith et al., 1988). We examine the relationship between the signs of diabetes and the risk factors using a GAM; therefore, the response variable Y_i indicates the presence of diabetes (0: negative, 1: positive). For each subject i , the predictor variables (risk factors) are $pregnant_i$ (number of times the subject was pregnant) $glucose_i$ (plasma glucose concentration in two hours in an oral glucose tolerance test [mg/dl]), $pressure_i$ (diastolic blood pressure [mm/Hg]), $triceps_i$ (triceps skin fold thickness [mm/Hg]), $mass_i$ (body mass index, BMI), $pedigree_i$ (diabetes pedigree function), and age_i (age).

To examine the relationship between Y_i and the risk factors, we consider the following GAM with a logit link,

$$\log \frac{E(Y_i)}{1 - E(Y_i)} = \alpha + f_1(pregnant_i) + f_2(glucose_i) + f_3(pressure_i) + f_4(triceps_i) + f_5(mass_i) + f_6(pedigree_i) + f_7(age_i). \quad (22)$$

The subjects with missing values are removed from the analysis. The results are summarized in Table 2 and Figure 13. The results are largely consistent with the intuition. Many variables have near-linear effects but a few variables clearly have nonlinear effects, for example, *mass* and *age*. The predictor variables with near-linear effects may instead be modeled using linear functions to reduce model complexity.

G R package GAMBMS

Here, we show how to use the R package for the BMS-based approaches for GAMs. Using the `devtools` package available at CRAN, our R package can be installed and loaded by running the following code:

```
devtools::install_github("hun-learning94/gambms")
library(gambms)
```

One can reproduce the results given in Sections 5 and F by running the examples in the help page of the R function `gambms`.

References

Al-Awadhi, F., Hurn, M., and Jennison, C. (2004). Improving the acceptance rate of reversible jump MCMC proposals. *Statistics & Probability Letters*, 69(2):189–198.

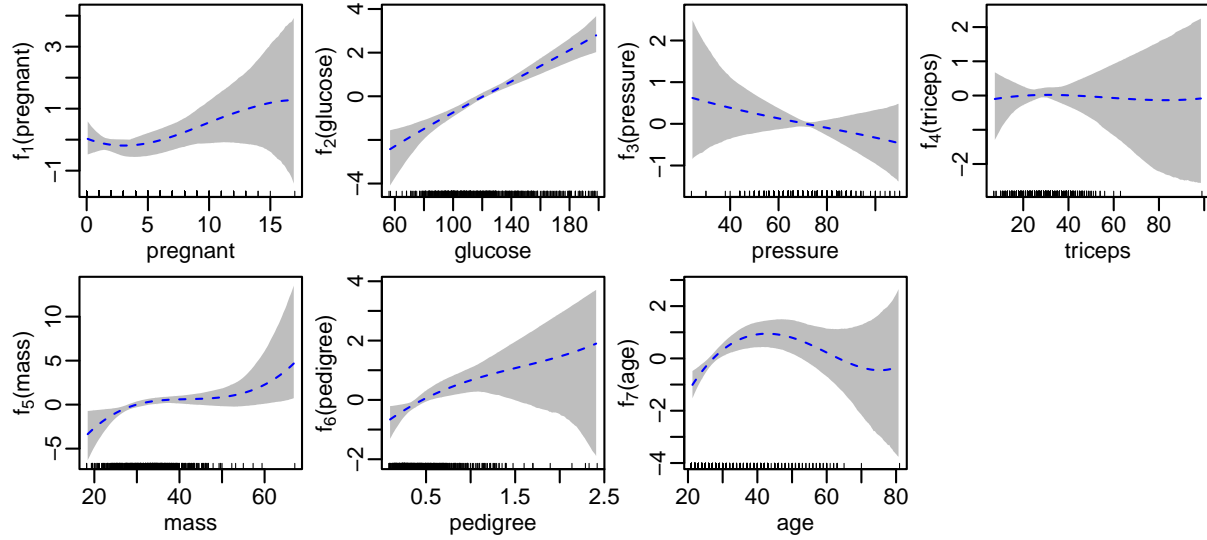


Figure 13: Pointwise posterior mean (blue dashed curve) and pointwise 95% credible band (gray shade) of the functions for the model in (22).

Albert, J. H. and Chib, S. (1993). Bayesian analysis of binary and polychotomous response data. *Journal of the American Statistical Association*, 88(422):669–679.

Antoniadis, A. (1997). Wavelets in statistics: a review. *Journal of the Italian Statistical Society*, 6(2):97–130.

Armero, C. and Bayarri, M. (1994). Prior assessments for prediction in queues. *Journal of the Royal Statistical Society: Series D (The Statistician)*, 43(1):139–153.

Bayarri, M. J., Berger, J. O., Forte, A., and García-Donato, G. (2012). Criteria for Bayesian model choice with application to variable selection. *The Annals of Statistics*, 40(3):1550–1577.

Berger, J. O., Pericchi, L. R., and Varshavsky, J. A. (1998). Bayes factors and marginal distributions in invariant situations. *Sankhyā: The Indian Journal of Statistics, Series A*, pages 307–321.

Brezger, A. and Lang, S. (2006). Generalized structured additive regression based on Bayesian P-splines. *Computational Statistics & Data Analysis*, 50(4):967–991.

Buhmann, M. D. (2003). *Radial Basis Functions: Theory and Implementations*, volume 12. Cambridge university press.

Chan, D., Kohn, R., Nott, D., and Kirby, C. (2006). Locally adaptive semiparametric estimation of the mean and variance functions in regression models. *Journal of Computational and Graphical Statistics*, 15(4):915–936.

Chen, M.-H. and Ibrahim, J. G. (2003). Conjugate priors for generalized linear models. *Statistica Sinica*, pages 461–476.

- Chipman, H. A., George, E. I., and McCulloch, R. E. (2010). BART: Bayesian additive regression trees. *The Annals of Applied Statistics*, 4(1):266–298.
- Cox, D. and Snell, E. (1989). *The Analysis of Binary Data*, volume 32. CRC Press.
- Crainiceanu, C. M., Ruppert, D., Carroll, R. J., Joshi, A., and Goodner, B. (2007). Spatially adaptive Bayesian penalized splines with heteroscedastic errors. *Journal of Computational and Graphical Statistics*, 16(2):265–288.
- Cripps, E., Carter, C., and Kohn, R. (2005). Variable selection and covariance selection in multivariate regression models. *Handbook of Statistics*, 25:519–552.
- Cui, W. and George, E. I. (2008). Empirical Bayes vs. fully Bayes variable selection. *Journal of Statistical Planning and Inference*, 138(4):888–900.
- De Boor, C. (1978). *A Practical Guide to Splines*, volume 27. springer-verlag New York.
- De Jonge, R. and Van Zanten, J. (2012). Adaptive estimation of multivariate functions using conditionally Gaussian tensor-product spline priors. *Electronic Journal of Statistics*, 6:1984–2001.
- Dellaportas, P., Forster, J. J., and Ntzoufras, I. (2002). On Bayesian model and variable selection using MCMC. *Statistics and Computing*, 12(1):27–36.
- Denison, D., Mallick, B., and Smith, A. (1998a). Automatic Bayesian curve fitting. *Journal of the Royal Statistical Society: Series B (Statistical Methodology)*, 60(2):333–350.
- Denison, D. G., Mallick, B. K., and Smith, A. F. (1998b). Bayesian MARS. *Statistics and Computing*, 8(4):337–346.
- DiMatteo, I., Genovese, C. R., and Kass, R. E. (2001). Bayesian curve-fitting with free-knot splines. *Biometrika*, 88(4):1055–1071.
- Fahrmeir, L. and Lang, S. (2001). Bayesian inference for generalized additive mixed models based on Markov random field priors. *Journal of the Royal Statistical Society: Series C (Applied Statistics)*, 50(2):201–220.
- Fouskakis, D., Ntzoufras, I., and Perrakis, K. (2018). Power-expected-posterior priors for generalized linear models. *Bayesian Analysis*, 13(3):721–748.
- Francom, D. and Sansó, B. (2020). BASS: An R package for fitting and performing sensitivity analysis of Bayesian adaptive spline surfaces. *Journal of Statistical Software*, 94(LA-UR-20-23587).
- Francom, D., Sansó, B., Kupresanin, A., and Johannesson, G. (2018). Sensitivity analysis and emulation for functional data using Bayesian adaptive splines. *Statistica Sinica*, pages 791–816.
- Gordy, M. B. (1998a). Computationally convenient distributional assumptions for common-value auctions. *Computational Economics*, 12(1):61–78.

- Gordy, M. B. (1998b). A generalization of generalized beta distributions. Division of Research and Statistics, Division of Monetary Affairs, Federal Reserve Boards.
- Green, P. J. (1995). Reversible jump Markov Chain Monte Carlo computation and Bayesian model determination. *Biometrika*, 82(4):711–732.
- Gressani, O. and Lambert, P. (2021). Laplace approximations for fast Bayesian inference in generalized additive models based on P-splines. *Computational Statistics & Data Analysis*, 154:107088.
- Guisan, A., Edwards Jr, T. C., and Hastie, T. (2002). Generalized linear and generalized additive models in studies of species distributions: setting the scene. *Ecological Modelling*, 157(2-3):89–100.
- Gupta, A. K. and Nadarajah, S. (2004). *Handbook of Beta Distribution and Its Applications*. CRC press.
- Gupta, M. and Ibrahim, J. G. (2009). An information matrix prior for Bayesian analysis in generalized linear models with high dimensional data. *Statistica Sinica*, 19(4):1641–1663.
- Gustafson, P. (2000). Bayesian regression modeling with interactions and smooth effects. *Journal of the American Statistical Association*, 95(451):795–806.
- Hansen, M. H. and Yu, B. (2003). Minimum description length model selection criteria for generalized linear models. *Lecture Notes-Monograph Series*, pages 145–163.
- Hastie, T. and Tibshirani, R. (1986). Generalized additive models. *Statistical Science*, pages 297–318.
- Hastie, T., Tibshirani, R., Friedman, J. H., and Friedman, J. H. (2009). *The Elements of Statistical Learning: Data Mining, Inference, and Prediction*, volume 2. Springer.
- Held, L., Sabanés Bové, D., and Gravestock, I. (2015). Approximate Bayesian model selection with the deviance statistic. *Statistical Science*, pages 242–257.
- Humbert, P. (1922). IX.—The confluent hypergeometric functions of two variables. *Proceedings of the Royal Society of Edinburgh*, 41:73–96.
- Jeong, S., Park, M., and Park, T. (2017). Analysis of binary longitudinal data with time-varying effects. *Computational Statistics & Data Analysis*, 112:145–153.
- Jeong, S. and Park, T. (2016). Bayesian semiparametric inference on functional relationships in linear mixed models. *Bayesian Analysis*, 11(4):1137–1163.
- Jeong, S., Park, T., and van Dyk, D. A. (2022). Bayesian model selection in additive partial linear models via locally adaptive splines. *Journal of Computational and Graphical Statistics*, 31(2):324–336.
- Ji, C. and Schmidler, S. C. (2013). Adaptive Markov Chain Monte Carlo for Bayesian variable selection. *Journal of Computational and Graphical Statistics*, 22(3):708–728.

- Jullion, A. and Lambert, P. (2007). Robust specification of the roughness penalty prior distribution in spatially adaptive Bayesian P-splines models. *Computational Statistics & Data Analysis*, 51(5):2542–2558.
- Kass, R. E. and Raftery, A. E. (1995). Bayes factors. *Journal of the American Statistical Association*, 90(430):773–795.
- Kass, R. E. and Wasserman, L. (1995). A reference Bayesian test for nested hypotheses and its relationship to the Schwarz criterion. *Journal of the American Statistical Association*, 90(431):928–934.
- Katznelson, Y. (2004). *An Introduction to Harmonic Analysis*. Cambridge University Press.
- Kohn, R., Smith, M., and Chan, D. (2001). Nonparametric regression using linear combinations of basis functions. *Statistics and Computing*, 11(4):313–322.
- Lang, S. and Brezger, A. (2004). Bayesian P-splines. *Journal of Computational and Graphical Statistics*, 13(1):183–212.
- Ley, E. and Steel, M. F. (2012). Mixtures of g-priors for Bayesian model averaging with economic applications. *Journal of Econometrics*, 171(2):251–266.
- Li, Y. and Clyde, M. A. (2018). Mixtures of g-priors in generalized linear models. *Journal of the American Statistical Association*, 113(524):1828–1845.
- Liang, F., Paulo, R., Molina, G., Clyde, M. A., and Berger, J. O. (2008). Mixtures of g priors for Bayesian variable selection. *Journal of the American Statistical Association*, 103(481):410–423.
- Magee, L. (1990). R^2 measures based on Wald and likelihood ratio joint significance tests. *The American Statistician*, 44(3):250–253.
- Maruyama, Y. and George, E. I. (2011). Fully Bayes factors with a generalized g-prior. *The Annals of Statistics*, 39(5):2740–2765.
- McLean, M. W., Hooker, G., Staicu, A.-M., Scheipl, F., and Ruppert, D. (2014). Functional generalized additive models. *Journal of Computational and Graphical Statistics*, 23(1):249–269.
- Nagelkerke, N. J. (1991). A note on a general definition of the coefficient of determination. *Biometrika*, 78(3):691–692.
- Nott, D. J. and Kohn, R. (2005). Adaptive sampling for Bayesian variable selection. *Biometrika*, 92(4):747–763.
- Park, T. and Jeong, S. (2018). Analysis of Poisson varying-coefficient models with autoregression. *Statistics*, 52(1):34–49.
- Rivoirard, V. and Rousseau, J. (2012). Posterior concentration rates for infinite dimensional exponential families. *Bayesian Analysis*, 7(2):311–334.

- Rossell, D., Abril, O., and Bhattacharya, A. (2021). Approximate Laplace approximations for scalable model selection. *Journal of the Royal Statistical Society: Series B (Statistical Methodology)*, 83(4):853–879.
- Sabanés Bové, D. and Held, L. (2011). Hyper- g priors for generalized linear models. *Bayesian Analysis*, 6(3):387–410.
- Sabanés Bové, D., Held, L., and Kauermann, G. (2015). Objective Bayesian model selection in generalized additive models with penalized splines. *Journal of Computational and Graphical Statistics*, 24(2):394–415.
- Scheipl, F. and Kneib, T. (2009). Locally adaptive Bayesian P-splines with a Normal-Exponential-Gamma prior. *Computational Statistics & Data Analysis*, 53(10):3533–3552.
- Schmidt, D. F. and Makalic, E. (2020). Bayesian generalized horseshoe estimation of generalized linear models. In *Joint European Conference on Machine Learning and Knowledge Discovery in Databases*, pages 598–613. Springer.
- Scott, J. G. and Berger, J. O. (2010). Bayes and empirical-Bayes multiplicity adjustment in the variable-selection problem. *The Annals of Statistics*, pages 2587–2619.
- Shen, W. and Ghosal, S. (2015). Adaptive Bayesian procedures using random series priors. *Scandinavian Journal of Statistics*, 42(4):1194–1213.
- Smith, J. W., Everhart, J. E., Dickson, W., Knowler, W. C., and Johannes, R. S. (1988). Using the ADAP learning algorithm to forecast the onset of diabetes mellitus. In *Proceedings of the Annual Symposium on Computer Application in Medical Care*, page 261. American Medical Informatics Association.
- Smith, M. and Kohn, R. (1996). Nonparametric regression using Bayesian variable selection. *Journal of Econometrics*, 75(2):317–343.
- Sohn, J., Jeong, S., Cho, Y., and Park, T. (2022). Functional clustering methods for binary longitudinal data with temporal heterogeneity. *arXiv preprint arXiv:2210.10273*.
- Umlauf, N., Adler, D., Kneib, T., Lang, S., and Zeileis, A. (2012). Structured additive regression models: An R interface to BayesX. Technical report, Working Papers in Economics and Statistics.
- Wang, L., Liu, X., Liang, H., and Carroll, R. J. (2011). Estimation and variable selection for generalized additive partial linear models. *Annals of Statistics*, 39(4):1827.
- Williams, C. and Rasmussen, C. (1995). Gaussian processes for regression. *Advances in Neural Information Processing Systems*, 8.
- Womack, A. J., León-Novelo, L., and Casella, G. (2014). Inference from intrinsic Bayes’ procedures under model selection and uncertainty. *Journal of the American Statistical Association*, 109(507):1040–1053.

- Wood, S. N. (2017). *Generalized Additive Models: an Introduction with R*. CRC press.
- Wood, S. N., Goude, Y., and Shaw, S. (2015). Generalized additive models for large data sets. *Journal of the Royal Statistical Society: Series C (Applied Statistics)*, 64(1):139–155.
- Yee, T. W. and Mitchell, N. D. (1991). Generalized additive models in plant ecology. *Journal of Vegetation Science*, 2(5):587–602.
- Yee, T. W. and Wild, C. (1996). Vector generalized additive models. *Journal of the Royal Statistical Society: Series B (Methodological)*, 58(3):481–493.
- Zellner, A. (1986). On assessing prior distributions and Bayesian regression analysis with g-prior distributions. *Bayesian Inference and Decision Techniques: Essays in Honor of Bruno de Finetti*, pages 233–243.
- Zellner, A. and Siow, A. (1980). Posterior odds ratios for selected regression hypotheses. *Trabajos de Estadística Y de Investigación Operativa*, 31(1):585–603.